KUOPION YLIOPISTON JULKAISUJA A. FARMASEUTTISET TIETEET 68
KUOPIO UNIVERSITY PUBLICATIONS A. PHARMACEUTICAL SCIENCES 68

OSSI KORHONEN

Starch acetate as a novel tablet excipient for extended oral drug delivery

Doctoral dissertation

To be presented by permission of the Faculty of Pharmacy of the University of Kuopio for public examination in Auditorium, Mediteknia building, University of Kuopio, on Monday 26th January 2004, at 12 noon

Department of Pharmaceutics
Faculty of Pharmacy
University of Kuopio

KUOPION YLIOPISTO
KUOPIO 2004

Distributor:
Kuopio University Library
P.O. Box 1627
FIN-70211 KUOPIO
FINLAND
Tel. +358 17 163 430
Fax +358 17 163 410
http://www.uku.fi/kirjasto/julkaisutoiminta/julkmyyn.html

Series Editor:
Eero Suihko, Ph.D.
Department of Pharmaceutics

Author's address:
Department of Pharmaceutics
University of Kuopio
P.O. Box 1627
FIN-70211 KUOPIO
FINLAND
Tel. +358 17 162 458
Fax +358 17 162 252
Email: ossi.korhonen@uku.fi

Supervisors:
Professor Jarkko Ketolainen, Ph.D.
Department of Pharmaceutics
University of Kuopio

Docent Petteri Paronen, Ph.D.
Department of Pharmaceutics
University of Kuopio

Reviewers:
Professor Henderik W. Frijlink, Ph.D.
Department of Pharmaceutical Technology and
Biopharmacy
University of Groningen
The Netherlands

Professor Martti Marvola, Ph.D.
Faculty of Pharmacy
University of Helsinki
Finland

Opponent:
Professor Anne Juppo, Ph.D.
Faculty of Pharmacy
University of Helsinki
Finland

ISBN 951-781-286-8
ISSN 1235-0478

Kopijyvä
Kuopio 2004
Finland

Korhonen, Ossi. Starch acetate as a novel tablet excipient for extended oral drug delivery. Kuopio University Publications A. Pharmaceutical Sciences 68. 2004. 94 p.
ISBN 951-781-286-8
ISSN 1235-0478

ABSTRACT

Oral administration is the most common form of drug administration, due to its good patient acceptance. To develop good quality, safe and potent drug delivery products requires an enormous amount of research on excipents and formulation design. The aim of this study was to evaluate the applicability of a novel starch acetate excipient for extended oral drug delivery.

Physicochemical properties of a starch acetate product having different degrees of substitution were studied. Effects of different drying methods on particle and powder properties and subsequent compactability were evaluated. Furthermore, release of different drugs from starch acetate tablets was analysed by multivariate data analyses. Finally, *in vivo* human studies were carried out to confirm the extended drug release characteristics of starch acetate tablets, and an *in vitro – in vivo* correlation was established using a novel direct cumulative under the curve approach.

Measured properties of the starch acetate were found to depend on the degree of acetate substitution. Starch acetate was found to be an amorphous polymer, where hydrophobicity increased as the degree of acetate substitution increased. The mechanical strength of tablets increased, and extended drug release could be found as the degree of acetate substitution increased. Using different drying methods, characteristics of particle, powder and consequent tableting properties could be affected. In particular, particles of different size, shape and surface properties could be produced. Drug release mechanisms from starch acetate tablets varied from Fickian diffusion to anomalous or even zero-order drug release, according to Power Law equation. As the release mechanism changed toward zero-order drug release, the lamination or cracking of the starch acetate tablet matrix became more dominant. Starch acetate was able to control the drug release rate between tablets with a desired drug. According to multivariate data analyses, molecule properties such as flexibility, hydrogen bonding capacity and molecular size parameters had a great impact on drug release kinetics and diffusional rate constants from starch acetate tablets. Factors that described tablet structure, and especially elasticity of the matrix, were identified as predictors of drug release rates in zero-order drug release. *In vivo* human studies confirmed that starch acetate could act as a release controlling excipient. An alternative approach was found to establish *in vitro-in vivo* correlation (IVIVC) as a predictable method for describing the correlation between the *in vitro* drug release and *in vivo* plasma concentration of diltiazem.

In conclusion, the present study demonstrated that novel starch acetate as an excipient can act as a release-controlling agent in extended oral drug delivery systems. It can be used as a direct compression excipient, and it allows for the formulation of drug release profiles in a simple way.

National Library of Medicine Classification: QV 800, QV 787, WB 350, QU 83
Medical Subject Headings: excipients; drug delivery systems; administration, oral; polymers; starch / analogs & derivatives; powders; tablets; multivariate analysis; pharmacokinetics; biological availability.

To My Family

ACKNOWLEDGEMENTS

The present study was carried out in the Department of Pharmaceutics, University of Kuopio, during the years 1997-2003.

I wish to express my sincere gratitude towards my principal supervisor, Professor Jarkko Ketolainen, Ph.D. It was Jarkko who opened this door to the world of academic science. He has been both forbearing and sympathetic in his guidance. I also owe my warmest thanks to my second supervisor, Professor and former Rector of the University of Kuopio and today's Mayor of Kuopio, Petteri Paronen, Ph.D. My sincere thanks also go to my part time supervisor, Professor Mika Vidgren, Ph.D. All of my supervisors have a strong intuition for pharmaceutical research. Thus, I feel that I have been in a privileged position during these years.

I wish to thank Professor Jukka Mönkkönen, Dean of the Faculty of Pharmacy, and Professor Jukka Gynther, former Dean of the Faculty of Pharmacy, for providing excellent facilities and working environment. My special thanks go to Professor Arto Urtti Ph.D., Head of the Department of Pharmaceutics and Professor Antti Poso, Ph.D. and Professor Kristiina Järvinen Ph.D., for their fruitful discussions.

My sincere thanks go to the official reviewers; Professor Henderik W. Frijlink, Ph.D., and Professor Martti Marvola, Ph.D., for their critical and valuable comments on this manuscript. I am very honoured that Professor Anne Juppo, Ph.D. accepted the invitation to be the opponent of my dissertation on the occasion of its public examination.

I warmly wish to thank my co-authors Seppo Pohja, M.Sc., Soili Peltonen, Ph.Lic., Pasi Raatikainen, Ph.D., Johanna Nakari, M.Sc., and Päivi Harjunen, M.Sc. Especially, I wish to acknowledge my closest colleague Eero Suihko, Ph.D., for those everyday discussions and for many practical things. Furthermore, I also thank our research group; Bert van Veen, Ph.D., Maarit Tarvainen, M.Sc., Pauliina Ahokanto, M.Sc., and Riikka Mäki, M.Sc., for helpful collaboration and friendship during these years. In addition, my many thanks go to Ms. Pirjo Hakkarainen, Mrs. Mirja Simonen, and Mrs. Päivi Tiihonen for their skillful technical assistance and friendship. I am grateful to all of the personnel of the Department of Pharmaceutics and the entire Faculty of Pharmacy.

Docent James Callaway, Ph.D, is gratefully acknowledged for revising the language of this thesis.

My warm thanks go to all my many friends outside of the University. I have especially had many relaxing, and sometimes unforgettable, and thrilling moments with the members of the Mustapannu hunting club. Also, my two hunting dogs, Ako and Jermu, have kept me on the move all the time.

I wish to thank my parents for their wisdom in motivating me towards the significance of education in my youth, and their endless support during these years (Kiitos Isi ja Äiti).

Finally, I know that I am not able to thank enough to my dear wife Ritva-Liisa for her tremendous love and support. My loved children Meri, Aleksi, Valtteri, Rosa, Kasperi and Patrik; you all bring the greatest comfort and joy to my life. This work is dedicated to all of you.

This work has been financially supported by The National Technology Agency of Finland (TEKES), the Eemil Aaltonen Foundation, The Finnish Pharmacists' Association, the Kuopio University Fund and the Pharmacal Research Foundation, Finland.

Kuopio, January 2004

Ossi Korhonen

ABBREVIATIONS

A	surface area
AUC	area under the plasma curve
$AUC_{0\text{-}24h}$	area under the plasma curve between 0 and 24 hours
$AUC_{0\text{-}\infty}$	area under the plasma curve between 0 and infinity
AUCcum(t)	cumulative area under the plasma curve at time t
AcN	acetonitrile
BCS	Biopharmaceutical Classification System
c	concentration of drug
c_s	drug solubility in polymer
C(t)	impulse response in convolution
$C_\delta(t)$	unit impulse response in convolution
C	volume reduction during tapping
C_s	solubility of drug
C_{max}	maximum plasma concentration
C_{min}	minimum plasma concentration in repeated dosing
D	diffusion coefficient
d	diameter
D_p	relative density at the compression pressure P
D_0	relative density because of die filling
D_b	relative density in particle rearrangement phase
D_A	$D_0 + D_b$
D(v, 0.1)	particle volume sizes in microns at which 10% of the sample is smaller
D(v, 0.5)	particle volume sizes in microns at which 50% of the sample is smaller
D(v, 0.9)	particle volume sizes in microns at which 90% of the sample is smaller
DCP	dicalcium phosphate dihydrate (Emcompress®)
DR	dissolution rate
Ds	amount of drug (mg) divided by tablet surface area (mm^2)
DSC	differential scanning calorimetry
ds	degree of substitution
EMEA	The European Agency for the Evaluation of Medical Products
ER%	elastic recovery
F	force
FDA	Food and Drug Administration, Centre for Drug Evaluation and Research
Flex	flexibility of drug
FW	molecular weight
FW/F	relative flexibility (ratio of FW and Flex)
f(t)	input function in convolution
F_{up}	maximum force of upper punch

F_{lo}	maximum force of lower punch
F_{ej}	maximum force of ejection
GI-tract	gastrointestinal tract
h	thickness
h_c	height
HPMC	hydroxypropylmethylcellulose
h_i	residual of observation I
H_{min}	minimum height of tablet during compression
H_{24}	tablet height 24 hours after tableting
HBAo	number of hydrogen acceptor oxygen atoms
HBD	the sum of hydrogen atoms bond to oxygen and to nitrogen atoms
HB	total amount of hydrogen bonding atoms
i.v.	intravenous
IVIVC	*in vitro* *in vivo* correlation
J	flux
Kh	square root of time drug release rate constant
Kz	zero-order drug release rate constant
k	release rate constant incorporating the matrix structure
Log P	partition coefficient of neutral molecule
Log D(6.8)	partition coefficient of molecule at pH 6.8
MCC	microcrystalline cellulose (Avicell PH101®)
M_t	amount of drug released at time t
M_∞	amount of drug released at time t=∞
MDT	mean dissolution time
MRT	mean residence time
MS	modified starch (Starch 1500®)
MV	molecular volume
m	mass
N	number of taps
n	diffusional exponent
P	pressure
PA	parachor
P_y	yield pressure
PC	principal component
PCA	principal component analysis
PC1	first principal component
PC2	second principal component
p_1	loading vector of first principal component in X-space
p_2	loading vector of second principal component in X-space
pK_a	ionisation constant
PO	polarization
PLS	partial least squares to latent structures
Q^2	goodness of prediction
Q_{60}	amount of dissolved drug at a particular time (e.g., 60 min)

r^2	goodness of model
r	radius of circle, cylinder, sphere or the half-thickness of a slab
SEM	scanning electron micrographs
Span	particle size distribution
S(g/l)	drug water solubility at pH 6.8
SSA	specific surface area
$T_{50\%}$	time required for dissolution of a fixed amount (50%)
TFA	trifluoroacetic acid
Td	tablet density
Tp	tablet porosity
Tm	tablet weight
T_{max}	time at maximum plasma concentration
tan θ	angle of repose
t	time
T_g	glass transition temperature
t_i	score value of observation i in X-space
t_1	score vector after first principal component in X-space
t_{i1}	score value of observation *i* in X-space
t_2	score vector after second principal component in X-space
u_{i1}	score value of observation i in Y-space (1 = first component)
u_1	score vector after first principal component in Y-space
u_2	score vector after second principal component in Y-space
USP	United State Pharmacopea
V	volume
V_0	loose volume of the powder column before tapping
V_N	volume of the powder column after a certain number of tapping (N)
VIP	variable importance on projection
w*c(1)	X- and Y-weight vectors after first principal component
w*c(2)	X- and Y-weight vectors after second principal component
W_{up}	upper punch work
W_{lo}	lower punch work
W_{exp}	expansion work
W_{eje}	ejection work
W_{fri}	friction work ($W_{fri} = W_{up} - W_{lo}$)
W_{net}	net work ($W_{net} = W_{up} - W_{exp} - W_{fri}$)
W_{rlo}	relative lower punch work (ratio of W_{lo} and W_{up})
W_{rexp}	relative expansion work (ratio of W_{exp} and W_{up})
W_{reje}	relative ejection work (ratio of W_{eje} and W_{up})
W_{rfri}	relative friction work (ratio of W_{fri} and W_{up})
% (w/w)	weight / weight percentage
%PE	prediction error percent
δ	device thickness (cm)
σ	tensile strength
ε	tablet porosity

ρ_m	particle density

LIST OF THE ORIGINAL PUBLICATIONS

This doctoral dissertation is based on the following publications, referred to in the text by bolded Roman numerals **I-IV:**

I Ossi Korhonen, Pasi Raatikainen, Päivi Harjunen, Johanna Nakari, Eero Suihko, Soili Peltonen, Mika Vidgren, Petteri Paronen: Starch Acetates - Multifunctional Direct Compression Excipients.
Pharmaceutical Research 17: 1138-1143, 2000

II Ossi Korhonen, Seppo Pohja, Soili Peltonen, Eero Suihko, Mika Vidgren, Petteri Paronen, Jarkko Ketolainen: Effects of Physical Properties for Starch Acetate Powders on Tableting.
AAPS Pharmaceutical Science & Technology 3(4), 2002

III Ossi Korhonen, Antti Poso, Mika Vidgren, Petteri Paronen, Seppo Pohja, Jarkko Ketolainen: PCA- and PLS-analyses in evaluating drug release from starch acetate matrix tablets.
European Journal of Pharmaceutical Sciences, 2003, Submitted

IV Ossi Korhonen, Harri Kanerva, Mika Vidgren, Arto Urtti, Jarkko Ketolainen: Administration of Novel Starch Acetate – Diltiazem Controlled Release Tablets to Healthy Human Volunteers.
Journal of Controlled Release, 2003, Accepted for publication

CONTENTS

1 INTRODUCTION

In most cases, a tablet is the most desirable dosage form for human drug administration. The main advantages of dosing drugs in tablet form are the relatively simple production and patient acceptance, leading to good compliance and improved therapeutic efficacy. In the treatment of chronic diseases, once-a-day products with a constant drug release rate are desired. Many different technologies are under intensive investigation to reach this goal. Even so, the most commonly used approaches are still different kinds of matrix tablets, coated tablets and osmotic pumps prepared by natural or synthetic polymers. The main disadvantage in developing new formulations is that the preparation of a once-a-day product often demands sophisticated production technology. The most desired production method would be direct compression tableting, with as few excipients as possible, as it is a cheaper than complex processes.

Controlled drug delivery is defined as a technique or approach by which active chemicals are made available to a specified target at a rate and duration designed to accomplish an intended effect (Qiu and Zhang 2000). A typical controlled release system is designed to provide stabile drug levels in plasma with reduced fluctuation via slow drug release over an extended period of time.

Until the last decade, the optimisation of drug formulation has been accomplished through trial and error, which is resource consuming. Today, the development and optimisation of formulations are based on well-established scientific principles (Gabrielsson et al. 2002). Due to this, and also due to the complex nature of formulations and preparation technologies, traditional statistical methods have not been able to interpret complex data very well. More recently, advanced statistical data analysis tools have been developed to increase the understanding of subtle relationships between factors and responses. Multivariate data analysis is often used in many fields of industry. In pharmaceutical technology, however, it has been practically neglected, although it has been shown to be powerful tool for modelling and predicting certain characteristics in complicated systems.

In pharmaceutical development, it is very important to understand the applicability of a product in humans as early as possible. In this way, inefficient products can be identified and excluded, thus reducing research and development costs. Early *in vivo* studies can also facilitate the creation of an *in vitro – in vivo* correlation (IVIVC). By the help of predictive IVIVC, it can be estimated how the changes in *in vitro* properties affect *in vivo* properties without biological studies.

In the present study, a novel tablet excipent, starch acetate, was investigated as an extended drug release agent for once-a-day tablet product. These studies included the characterization of particle, powder and tableting properties, evaluation of *in vitro* drug release properties from a simple binary mixture of starch acetate-drug in direct compressed tablets using multivariate data analyses, administration of starch acetate – diltiazem hydrochloride tablets to the healthy human volunteers to evaluate pharmacokinetic parameters including, bioavailability and IVIVC.

2 BACKGROUND OF THE STUDY

In the starch acetate patent (Paronen et al. 1997), it was pointed out that starch acetate might be a very promising polymer excipient in the formulation of extended release products.

In this chapter, the most important factors in the pharmaceutical development of extended drug release products are introduced and taken into account. The basics of oral drug delivery, solubility of drug in gastrointestinal tract (GI-tract) and drug absorption from the GI-tract are first outlined. The basics of drying and its effect on particle and powder properties are also presented. The drug release mechanisms and theoretical background of multivariate data analysis (PCA and PLS) for the evaluation of *in vitro* drug release is introduced. Finally, *in vivo* pharmacokinetics and methods in the creation of *in vitro* *in vivo* correlation (IVIVC) are discussed.

These topics form the fundamental background for the development of pharmaceutical oral dosage forms. All these aspects must be kept in mind throughout the development process, making it complicated, but also challenging and interesting.

2.1 Oral drug delivery

It is estimated that even today approximately 90% of all medicines are taken in oral dosage forms. The market share of oral controlled release systems is currently about 3.5 billion USD, which is about half of the total annual controlled drug delivery market (Venkatraman et al. 2000). The often-mentioned advantage of oral delivery is good patient compliance. The patient is able to administer the oral dosage form independently, negating the need for skilled or expensive medical interventions.

The drug faces complex environmental conditions in the GI-tract, including extremes of pH, intestinal motility, mucus barriers, p-glycoprotein efflux systems, some metabolic activity and the bilayer of the membranes of the epithelium. After penetrating the gut wall, all drugs enter the systemic circulation via the liver, where a considerable portion of the delivered drug might be metabolised. Thus, before the development of oral drug delivery systems, the physiological and physicochemical aspects of the GI-tract are important to keep in mind.

2.1.1 Drug dissolution in the gastrointestinal tract

The basic assumption is that only the dissolved and neutral form of a drug is able to pass from the lumen of GI-tract into the systemic circulation, although there is some evidence that the small particles can also penetrate the GI-epithelium (Ebel 1990, Desai et al. 1996, Hussain et al. 2001). There exist some basic factors that have great influence on drug solubility and subsequent absorption by the GI-tract. The Noyes-Whitney equation (1897) (Eq. 1) is a fine rule of thumb for describing the important factors that are involved in the kinetics of drug dissolution in the GI-tract (Hörter and Dressman 2001):

$$DR = \left(\frac{D \cdot A}{V \cdot h} \right) \cdot (C_s - c) \tag{1}$$

where DR is the dissolution rate, D the diffusion coefficient of the drug, A the surface area available for dissolution, h the thickness of the boundary layer adjacent to the dissolving drug surface, V the volume of dissolution medium, C_s the solubility of the drug and c the concentration of dissolved drug.

Most therapeutic drugs are weak acids or bases; i.e., their solubility depends on their ionisation constants and the pH of the dissolution medium (Ozturk et al. 1988). The pH varies between different parts of GI-tract, thus the solubility of drug changes when it travels through GI-tract (Evans et al. 1988). It should be noted that the pH profile in the GI-tract can change also due to the different factors like age, diet, pathophysiological conditions or the administration of certain drugs such as proton pump inhibitors (Ovesen et al. 1986, Dressman et al. 1990, Russel et al. 1993, Sharma 1999). Fractional amount of ionized drug can be written from Henderson-Hasselbalch relationship for weak molecular acid as follows (Eq. 2):

$$\%Ionized = \frac{100}{(1 + anti\log(pK_a - pH))} \tag{2}$$

and for weak molecular base (Eq. 3):

$$\%Ionized = \frac{100}{(1 + anti\log(pH - pK_a))} \tag{3}$$

In addition, drug crystallinity/polymorphism/amorphicity (Shefter and Higuchi 1963, Haleblian and McCrone 1969, Yu 2001), the particle size of a drug (Atkinson et al. 1962, Jounela et al. 1975, Hintz and Johnsson 1989), the solubilization of a drug by natural surfactants (like bile salts) (Bates et al. 1966, Kassem et al. 1982, Luner et al. 1994, Mithani et al. 1996), different kinds of hydrogen acceptor/donor interactions (Rasool et al. 1991), the wetting processes of a drug (Bakatselou et al. 1991), the content and volume of the GI-tract (Macheras et al. 1990, Dressman et al. 1998) and the viscosity of the GI-fluid (Reppas et al. 1991) can all have their own specific impact on drug dissolution in GI-tract.

2.1.2 Drug absorption from the gastrointestinal tract

A drug faces different barriers during absorption from the lumen of GI-tract to the blood circulation (Norris et al. 1998). Thus, there exist different routes and mechanisms that are involved in drug permeation across these barriers.

The first physical barrier is mucus, which is mainly composed of water and glycoproteins (Strous and Dekker 1992). Mucus acts as a viscoelastic lubricant and protective layer upon the GI-tract epithelium. A drug must diffuse through this physiological barrier prior to reaching the absorbing surface. The diffusion rate depends on the thickness of the mucus layer, mucus viscosity and possible interactions between the drug and mucus.

When a drug has reached the absorbing surface, the surface of epithelium cells, it encounters a hydrophobic bilayer cell membrane. The cell membrane is a highly organized structure, composed of tightly packed lipid molecules with proteins, which act as structural elements, transporters and environmental monitors (Singer and Nicolson 1972).

In the transcellular transport, the cell membrane allows for the penetration of nonpolar and uncharged drugs (i.e., small, neutral and lipophilic drugs), but not polar or charged drugs (Egan and Lauri 2002). Thus, the transport of lipophilic drugs occurs through the bilayer of the membranes of the epithelium.

The paracellular route is possible diffusional pathway for small and hydrophilic drugs (Camenisch et al. 1996). The epithelial cells are bound together by different types of junctions, including desmosomes, gap junctions and junctional complexes that also serve as a route for drug absoption (Tanaka et al. 1995).

In facilitated diffusion, cell membrane transporters are involved (Tsuji and Tamai 1996). This is an active transport mechanism, which can transport drugs against diffusion gradient, as it is an energy-consuming process. These transport mechanisms are only applicable to drugs having a small molecular weight, typically under 500 Da. Larger molecules (even macromolecules) can be transported by endocytic prosesses, but the efficacy of endocytosis is much lower than diffusional processes.

In addition to these physiological barriers, there is also a biochemical barrier in drug absorption. The GI-tract contains many degradative enzymes that form a barrier for drug absorption (Dressman et al. 1998). The G-protein efflux system is included in this biochemical barrier (Stouch and Gudmundsson 2002, Schinkel and Jonker 2003). The fact is that the modification of drug absorption is very difficult, and thus the easier way is to affect drug dissolution in the GI-tract is by using different drug delivery systems.

2.2 Controlled oral drug delivery

According to Qiu and Zhang (2000) controlled release may be defined as a technique or approach by which active chemicals are made available to a specified target at a rate and duration designed to accomplish an intended effect. More specifically, an oral controlled drug delivery system is, in principle, a device or dosage form that controls drug release and absorption by the GI-tract. A typical controlled release system is designed to provide constant or nearly constant drug levels in plasma with reduced fluctuation via controlled drug release over an extended period of time.

Controlled release dosage forms (equivalent to modified release dosage form) include the following subclasses; extended release (equivalent to prolonged release), delayed release, pulsatile release and accelerated release dosage forms (EMEA 1999a). An extended release dosage form is defined as one with a slower release than that of the conventional release dosage form administered by the same route. In the case of delayed release, the release of an active substance is delayed for a predefined period after administration or application of the dosage form. Pulsatile release is the release of an active substance within predefined time intervals, which is achieved by an appropriate manufacturing method. Accelerated release is a special drug delivery system, where drug release is accelerated compared to conventional dosage form.

There are some principles that must be considered in deciding whether or not a drug is feasible in oral extended delivery systems (Qiu and Zhang 2000). A poorly water-soluble drug with a high dose requirement may be unsuitable for the controlled delivery

systems. The drug has to be stable to pH, enzymes and other environmental conditions existing in the GI-tract, and the drug must have sufficient cell membrane permeability properties in the entire GI-tract to become absorbed. The best result can be achieved with a drug having a short elimination half-life, but in the case of drugs owing half-lives above 17 hours, it makes no idea to develop a slow release formulation. Drugs having a narrow therapeutic index might be good candidates for controlled delivery systems, as extended drug release reduces the fluctuation of plasma concentrations. However, in the case of very serious adverse events upon undesired dose dumping of drug, it should never formulate an extended drug release product. The extended oral delivery system for drugs that experience high first-pass metabolism might be inapplicable, as slow drug release allows effective metabolism, which reduces plasma concentrations.

2.2.1 Polymers in matrix type oral drug delivery systems

Polymers are the most common excipients used to control or modify drug release from tablet dosage forms. Polymers for controlling drug release from oral drug delivery systems can be divided into natural polymers and their derivatives, and synthetic polymers. The chemical nature of these polymers varies remarkably. Because of that each polymer has its own particular drug release properties. Also, their applicability towards different controlled delivery systems varies.

The most common hydrophilic polymers in oral controlled delivery systems are derivatives of cellulose and starch, especially hydroxypropyl methylcellulose (HPMC) (Colombo 1993, Te Wierik et al. 1997). Other hydrophilic polymers are xantham gum (Talukdar and Kinget 1997), sodium alginate (Efentakis and Buckton 2002), and poly(ethylene oxide) (Kim 1995). The most typical characteristic property of these polymers is their high swelling capacity, which has a significant effect on drug release kinetics (Colombo 1993, Gao et al. 1996). Many commercial grades of these polymers are available. Hydrophobic polymers are rarely used as a matrix forming excipient. Typical hydrophobic polymers are ethylcellulose and ammoniomethacrylate copolymers (Eudragit®).

2.2.2 Release mechanisms

The study of drug release mechanisms is an essential part of the development process of controlled drug delivery systems. Depending the release mechanism, the factors that

control drug release varies. The main mechanisms are diffusional, swelling, degradation and polymer dissolution. In practice, each mechanism is involved in drug release to some extent, which makes the understanding and mathematical modelling of the drug release phenomenon very complicated.

2.2.2.1 Diffusion-controlled systems

Diffusion is a major phenomenon that is involved in drug release from a matrix system, but it rarely exists alone (Narasimhan 2000). In diffusion-controlled systems, a drug is incorporated in the polymer, either dissolved or dispersed, and the polymer phase can be a porous or nonporous system. The main points where it appears are during the water penetration into the matrix and the drug transport from the matrix. Essential factors controlling drug release are the aqueous solubility of a drug, initial drug concentration in the matrix, porosity, tortuosity of pores and additional polymer properties. The transport of a drug from a polymer matrix can be described by Fick's law of diffusion (Eq. 4).

$$J = -D\left(\frac{c}{\delta}\right) \tag{4}$$

where J is the molar flux of the drug (mol/cm^2 s), D a diffusion coefficient of drug in the polymer (cm^2/s), c the concentration of the drug (mol/cm^3), and δ the device thickness (cm). This equation assumes that the diffusion coefficient is constant. However, in the case of pharmaceutical drug delivery matrices, the diffusion coefficient is rarely constant, but depends factors such as drug concentration, temperature, pressure, solvent properties and the chemical nature of the solute (Martin 1993). In addition, the degree of crystallinity and swelling of the polymer, porosity, tortuosity, relaxational behaviour, and the geometry of the device should be taking into account in modelling drug release from diffusion based matrices.

2.2.2.2 Swelling-controlled system

Drug release from a swelling-controlled system is a very complex phenomenon, due to the complex macromolecular changes in the polymer during drug release. HPMC is the most common swelling-controlled polymer for the preparation of oral controlled

drug release systems (Colombo 1993), and thus, it is a good example of a swelling-controlled system.

According to Siepmann and Peppas (2001) and Siepmann et al. (2002), the following simplified phenomena are involved in drug release from HPMC matrix tablets; initially, water penetrates into the HPMC matrix due, to the high water concentration gradient at the polymer/water interface. This process is taken into account as; (I) the exact geometry of the tablet, (II) the axial and radial direction of the mass transport and (III) the significant dependence of the water diffusion coefficient on the matrix-swelling ratio. In addition, water acts as a plasticizer, which decreases the glass transition temperature of HPMC, thus allowing phase transition from the glassy to the rubbery state. The rubbery state allows for much greater mobility of the polymer chain than the glassy state, leading to higher mass transfer rates of water and drug. Water affects the swelling of HPMC, which increases the dimensions of a device, and subsequently the concentrations of both polymer and drug. Penetrating water dissolves the drug, which starts to diffuse out of the device due to a concentration gradient between the device and the surrounding dissolution medium. At the same time, increased water content in the system increases the diffusion coefficient of a drug. In the case of poor water-solubility, both dissolved and undissolved drug co-exist within the polymer matrix. Undissolved drug is not available for diffusion. In the case of high initial drug loadings, the inner structure of the matrix changes significantly during drug release, becoming more porous and less restrictive for diffusion upon drug depletion. Depending on the chain length and degree of substitution of the hydrophilic polymer, the polymer itself dissolves more or less rapidly. In addition of swelling and diffusion, the erosion of gelled polymer might be also occurred that has to be taken into account as an one of the determining factors in drug release.

Since the 1960s, the development of a valid mathematical model has been based on different theories to describe drug release from HPMC matrices (e.g. Hubert et al. 1966, Lapidus and Lordi 1966 and 1968, Peppas et al. 1980, Lee 1980, Peppas and Franson 1983, Lee and Peppas 1987, Harland et al. 1988, Lee and Kim 1991, Möckel and Lippold 1993, Tahara et al. 1995 and 1996, Ju et al. 1995a, 1995b, 1997). Because of this, it is quite impossible to describe in detail the entire development process in this context, but the most recent examples will be discussed briefly.

The "sequential layer" model was recently developed to describe drug release from HPMC-matrix tablets by Siepmann et al. (Siepmann et al. 1999a, Siepmann et al. 1999b, Siepmann et al. 2000a, Siepmann et al. 2000b, Siepmann et al. 2002). This

mathematical model is able to take into account the polymer dissolution, the effect of HPMC grade, type of drug, the initial drug loading, the effect of tablet dimensions, diffusion of water and drug, non-constant diffusitivies, moving boundaries and the swelling of a system. This model is based on many theories, such as the reptation theory in polymer dissolution (Narasimhan and Peppas 1996a, 1996b, 1997a, 1997b), Fick's second law in the diffusion of water and drug (Crank 1975), the free volume theory of diffusion in the water content of a system (Fujita 1961) and both axial and radial mass transport, and concentration-dependent diffusivities. However, the correct use of this model demands a very deep understanding of different theories and well-established research methodologies. This might hinder the utilization of this model, although it might be the most applicable and predictive model that is currently available to model drug release from controlled delivery systems.

2.2.2.3 Erosion and (bio)degradation controlled systems

Chemically controlled delivery systems are related to polymeric matrices, where drug diffusion is controlled by bioerosion or biodegradation. Chemical reactions that trigger drug release may include hydrolysis, enzymatic or biochemical mechanisms. According to Narasimhan (2000), bioerosion is a process where physiological fluids simply dissolve the polymer, rather than break it down. In the case of biodegradation, the polymer will break down, via chemical reactions, into small molecular weight fragments. In addition, the erosion can be divided into subcategories of surface and bulk erosions (Tamada and Langer 1993, Göpferich 1996). As the names of surface erosion implies out, erosion occurs on the surface of the polymer matrix. In bulk erosion, polymers degrade or erode throughout the matrix.

2.2.2.4 Polymer dissolution controlled systems

According to Narasimhan (2001), two processes are involved in the dissolution of a polymer. There are both solvent diffusion into the polymer and polymer chain disentanglement. To examine this, two cases are presented; namely amorphous polymers and semicrystalline polymers.

With amorphous polymers, a drug is molecularly dispersed into an amorphous polymer phase, which is usually in the glassy state (Narasimhan 2001). When a soluble polymer – drug matrix is placed into the dissolution medium, the solvent penetrates into

the matrix, causing a reduction in the glass transition temperature (T_g) of a polymer. Once the T_g equals the temperature of the system, the polymer starts to change from the glassy to the rubbery state and, consequently, it swells and forms a gel-like layer on the surface of the matrix. In semicrystalline polymer dissolution, it is assumed that dissolution follows the same mechanism as that of amorphous polymers but, at the beginning, the crystalline chains unfold and join to the amorphous state (Mallapragada and Peppas 1997).

2.3 Drying of solids

Most starting materials in pharmaceutical solids undergo drying at some production stage. The drying stage is the final step where the physical properties of solids can be modified. It has been pointed out that the drying conditions are of significant importance for both friability and bulk density (Remon and Schwartz 1987), surface structure and mechanical strength (Bataille et al. 1993, Dryer et al. 1994), porosity (Bataille et al. 1993, Kleinebudde 1994, Habib and Shangraw 1997), compaction properties (Chatrath and Staniforth 1990, Habib and Shangraw 1997) and drug release properties (Dryer et al. 1994). Although these studies have been carried out with granular systems, the results can be generalized to all bulk pharmaceuticals.

2.3.1 Mechanisms of drying

In drying, the basic goal is the removal of water from bulk solids. Evaporation of moisture occurs when the vapour pressure of the moisture on the solid surface is equal to the atmospheric pressure (Menon and Mujumdar 1987). It can be achieved by raising the temperature and/or lowering the pressure inside the dryer. If the pressure is lowered below the triple point and the temperature is correctly adjusted, the water directly sublimates from ice to water vapour, which is the case in freeze-drying. According to Menon and Mujumdar (1987), there are four methods of drying and these are based on methods of heat transfer; i.e. conduction, convection, radiant and dielectric heating.

Conduction is a suitable method for very wet solids (Menon and Mujumdar 1987). Heat for evaporation, usually hot water steam or hot oil, is supplied through a heated surface, where it is conducted to the solid. Often, appropriate mixing is added for the smooth distribution of heat. Evaporated moisture is carried away under vacuum. A more

powerful vacuum can be used for heat-sensitive solids. Typical conduction dryers are described as tray, rotary and drum dryers.

Convection is the most common way of drying solids (Menon and Mujumdar 1987). In convection, heat is supplied by a heated gas (normally air, but nitrogen is also possible), which causes the vaporization of water. The heat is effectively transferred from gas to solid by convection, which makes it a fast and powerful drying method. Typical convection dryers are fluid bed and spray dryers.

In the radiation method of drying, electromagnetic radiation at wavelengths between 0.2m – 0.2μm is exposed to the product, which causes warming (Menon and Mujumdar 1987). By selecting suitable wavelengths (e.g. microwaves), radiation penetrates to the water molecules, which causes the boiling and eventual evaporation of moisture. This is commonly used in modern household kitchens with the microwave oven. The radiation method is often connected with other drying methods.

Dielectric heating is a rarely seen method in drying (Chatrath and Staniforth 1990). In this concept, product is placed between two electrodes and a radio frequency radiation (27 MHz) is applied to the drying chamber.

It should be noted that the moisture content of a product is an equilibrium reaction. Thus, a product tends to be at equilibrium with the ambient humidity during storage, which consequently changes the properties of a solid.

2.4 Multivariate methods in controlled drug delivery

Until the last decade, optimizing formulation was primarily done through trial and error, which is very resource consuming. Today, the development and optimisation of formulation is accomplished through experimental desing (Gabrielsson et al. 2002). In addition, advanced statistical data analysis tools enhance the understanding of relationships between factors and responses (Karnachi and Khan 1996, Sastry et al. 1997, Takayama et al. 2000, Hamed and Sakr 2001).

As pointed out earlier, drug release from matrix tablets is a very complicated phenomenon to model and predict, due to the many factors affecting the release phenomenon. Thus, traditional data analysis methods are not able to cope with this task. Multi- and megavariate data analysis tools have been developed to manage large data matrices and complex relationships between variables and responses (Geladi and Kowalski 1986, Wold et al. 1987a and 1987b, Wold et al. 2001).

Multivariate data analyses, Principal Component Analysis (PCA) and Partial Least squares to latent Structures (PLS) have been successfully applied in many fields of research. For example, in the prediction of drug solubility and permeability through different biological membranes (Lindberg and Lundstedt 1995, Österberg and Norinder 2001, Weber et al. 2001, Bergström et al. 2002)

To date, PCA and PLS have only been utilized in a very few studies (12 papers according to Gabrielsson et al. 2002) in the field of pharmaceutical technology (e.g.; Zackrisson et al. 1995, Jover et al. 1996, Pinto et al. 1997, Westerhuis et al. 1997, Dyrstad et al. 1999, Adams et al. 2001, Tarvainen et al. 2001, Adams et al. 2002). In these few studies, the multivariate methods proved to be a very useful tool for modelling and predicting different pharmaceutical properties.

2.4.1 Basics of multivariate data analysis

Data always contains both systematic information about the system and noise (variability) (Wold et al. 2001). By using an appropriate analysis method, the systematic information can be extracted from the system. This noise is a mixture of measurement, experimental, sampling, modelling and some other errors, which are involved in all measurements and experiments. The noise affects the variability of data. Also, when the amount of variables increase, the complexity of data also increases, making the data multivariate. Subsequently, evaluation of the data by classical methods is difficult.

As the amount of variables increase, the independency of variables might be reduced (Eriksson et al. 2001). In classical data analysis (e.g.; regression analysis), the basic assumption is that all variables are totally independent, which means that one of two correlating variable has to be removed from the analysis, while multivariate data analyses are able to manage multiple correlating variables.

Individual measurements may contain large variability (noise), while important effects might be obscured (Eriksson et al. 2001). Multivariate projection methods are robust to noise in both the X data matrix and the Y response matrix, and they are able to filter data to highlight the real effects.

Multivariate projection methods are also able to handle data matrices that include missing data (Eriksson et al. 2001). If the resulting matrix contains around 50-100 observations, multivariate projection methods allow for 10-20 % of the missing data.

Based on the many advantages of multivariate data analyses, multivariate methods, especially PCA and PLS, are a promising tools for modeling and predicting drug release from matrix tablets.

2.4.2 Principal component analysis (PCA)

Principal component analysis (PCA) forms the basis for multivariate analysis (Wold et al. 1987a, Wold et al. 1987b). The PCA data matrix consists of observations in rows with variables in columns. The observations can be analytical samples and/or chemical compounds. The variables can be measurements that describe a system. The results may reveal groups of observations, trends and outliers. Prior to PCA, data is often pre-treated, as the numerical values of variables may have substantially different scales. This means that variables having different ranges also have different variances. In the pre-treatment, variances are normalized and, thus, the variables are given an equal weight in subseqvent calculations. The most common pre-treatment protocol includes unit-variance scaling and mean-centering (Fig. 1).

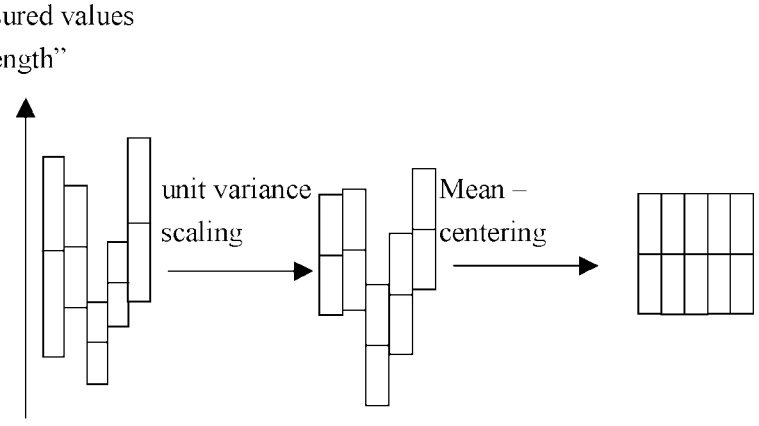

Figure 1. After unit-variance scaling and mean-centering all variables have the same length and the mean value is zero

According to Eriksson et al. (2001), the first principal component is a line in the variable space, which best approximates data in the least squares sense (Fig. 2). This line is the average point, which goes through the origin. After that, all observations can be projected onto this line, in order to get a co-ordinate value along the principal component line. This new co-ordinate value is known as a score (t).

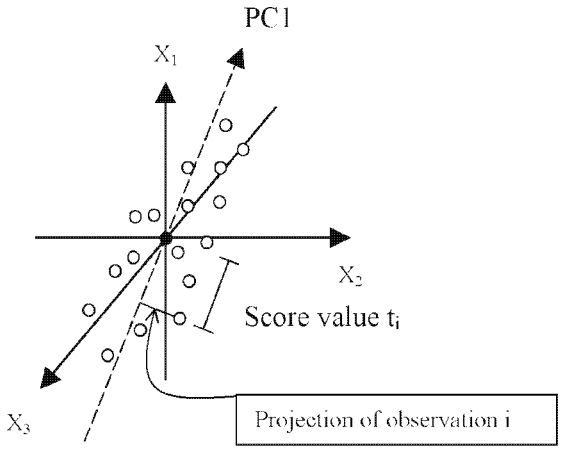

Figure 2. First principal component (PC1) is the line, which best describes the shape of the point swarm.

The second principal component is also a line, which is orthogonal to the first component and also passes through the origin (Fig. 3) (Eriksson et al. 2001). Together, these two components define a plane in the variable space. By projecting all observations onto this plane and plotting the co-ordinate values (score plot), it becomes possible to visualize the structure of the studied data set (Fig. 4). Observations that are close to each other in the PCA score plot (Group 1 in Figure 4) have similar properties, whereas observations far from each other are dissimilar, with respect to the studied properties.

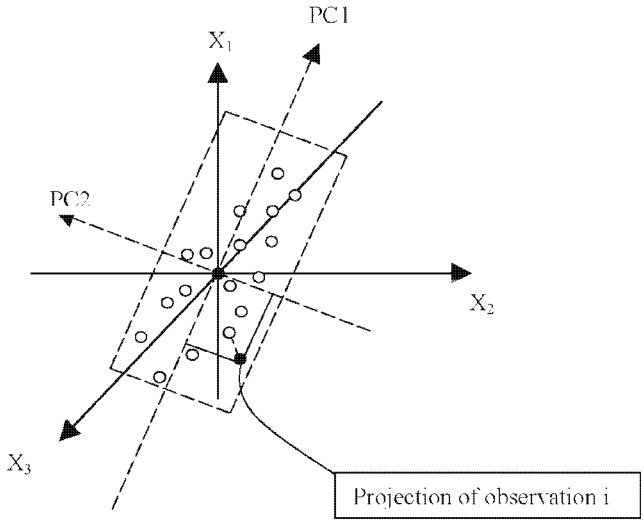

Figure 3. The second principal component (PC2) is orthogonal to PC1. It reflects the second largest amount of variation in the data.

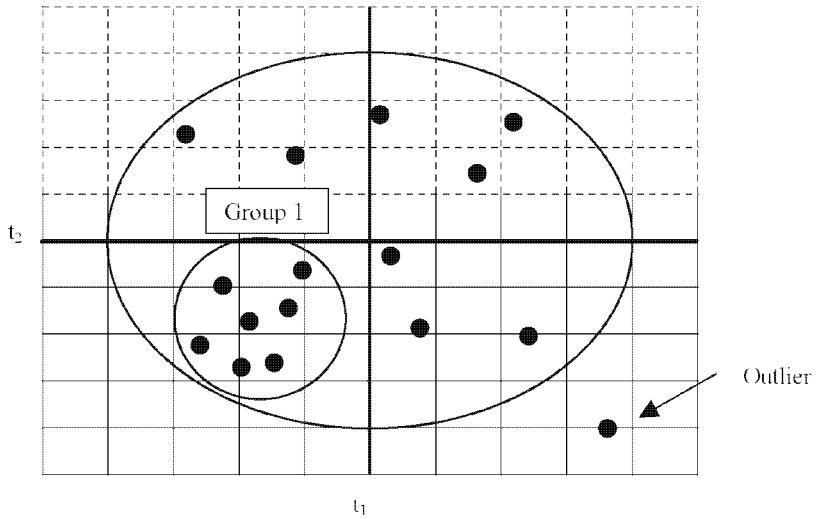

Figure 4. PCA score plot. Dots are observations, which are projected onto the PC1 versus PC2 score plot.

The meaning of scores is given by their loading (Eriksson et al. 2001). The loadings define the orientation of the principal component plane with respect to the original X-

variables. Algebraically, the loadings inform how the variables are linearly combined to form the scores. The loadings also tell about the magnitude (large or small correlation) and the manner (positive or negative correlation) in which the measured variables contribute to the scores. Thus, variables contributing similar information are grouped together (e.g.; variables 1, 2 and 3 in group A or variables 4 and 5 in group B) (Fig. 5), and they are positively correlated; e.g., as the numerical value of variable 1 increases or decreases, the numerical value of variable 2 and 3 tend to change in the same way. Inversely, variables between group A and B are negatively correlated, for example, when the numerical value of variable 1 in group A increases as the numerical value of variable 4 in the group B decreases.

In addition, the distance of variable to the plot origin indicates the magnitude of that variable. The further away a variable position lies from the origin, the stronger the impact that variable has on the model. Inversely, variable 6 lies near the origin and, thus, it has no effect on the model. Furthermore, loadings can be used to interpret the meaning of the scores. Group 1 (Fig. 4), for example, can as characterized as having high values for variables 1, 2 and 3, but low values for variables 4 and 5 (Fig. 4 and 5). So, from the PCA score and loading, groups of observations, trends, outliers and relationships can be seen between observations and variables.

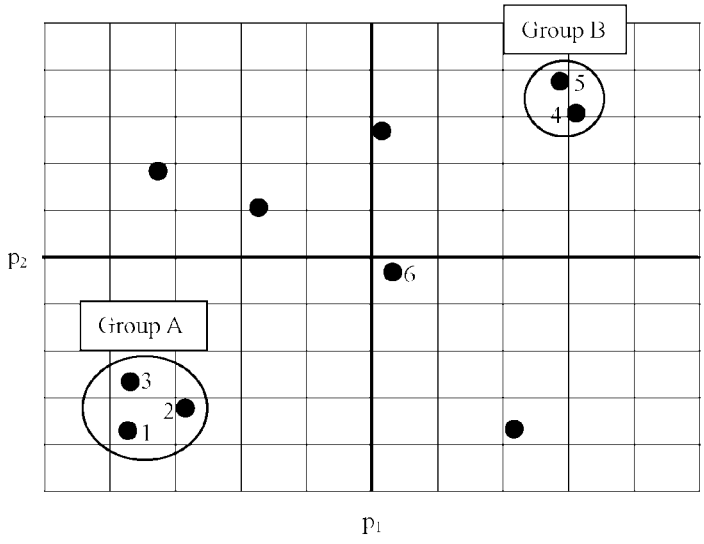

Figure 5. PCA loading plot. Dots are weights, which define the orientation of the plane in the variable space.

2.4.3 Partial least squares to latent structures (PLS)

PLS is a regression extension of PCA, which connects information in two blocks of variables; X and Y, (Wold et al. 2001, Eriksson et al. 2001). The main difference between PCA and PLS is that in PLS each row of a data table corresponds to two points rather than one; one in the X-space and one in the Y-space (response) (Fig. 6).

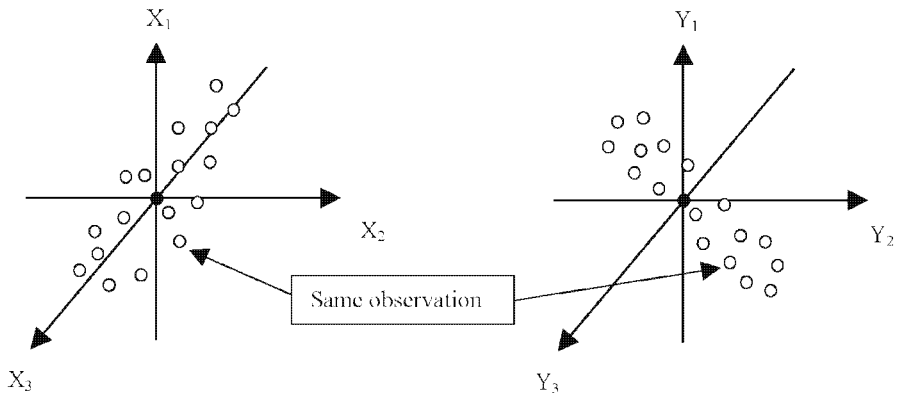

Figure 6. Observations are divided into two point-swarms; one in the predictor (X) space and one in the response (Y) space.

The first PLS component is a line an the X- and Y-coordinates that approximates the point-swarms, passing through the origins of each plot, and provides a good correlation with the score vector u_1. All observations are projected onto these lines in order to get the score vectors t_1 and u_1, for X and Y, respectively (Fig 7A and 7B). The X-score vector can be considered as a new variable, which reflects the information from the original X-variables. A correlation between X- and Y-space is achieved when the score vectors t_1 and u_1 are connected through inner relation (Eq. 5) (Fig. 7C):

$$u_{i1} = t_{i1} + h_i \qquad (5)$$

where u_{i1} is the score value of observation i in Y-space, t_{i1} the score value of observation i in X-space and h_i is a residual. Number 1 indicates the component number.

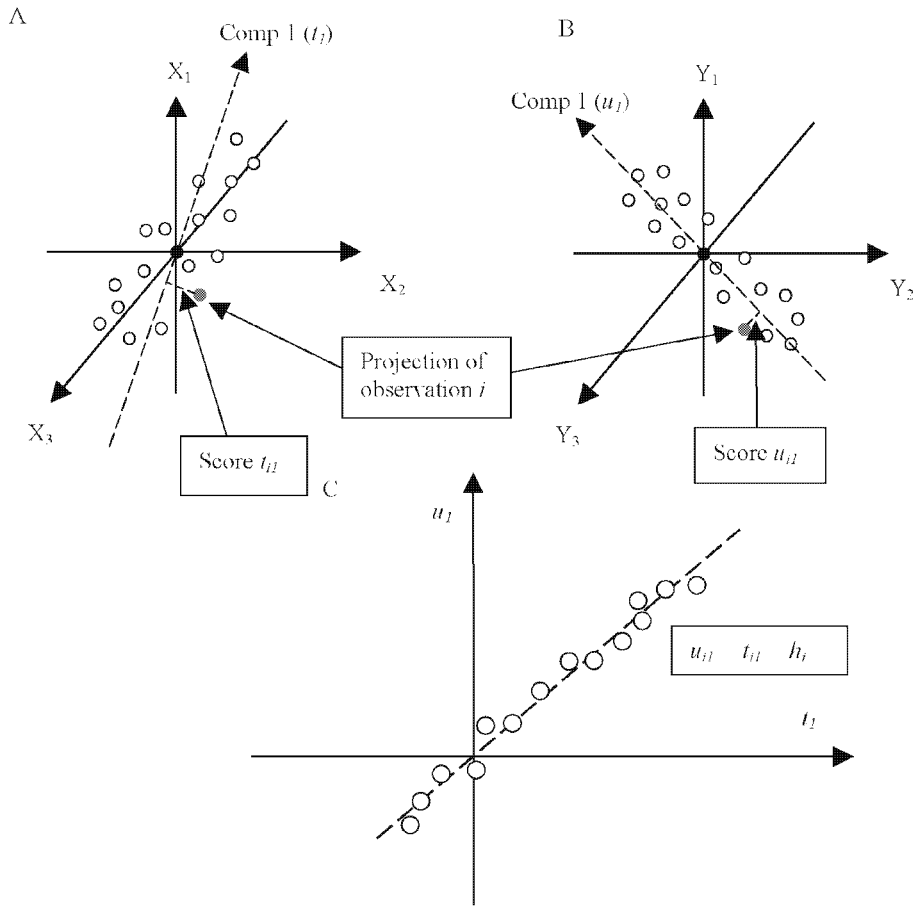

Figure 7. The first component of a PLS-model forms two lines, one in the X-space (A) and other in the Y-space (B). Information between X- and Y- spaces is connected and correlated through the inner relation ($u_{i1} - t_{i1} \mid h_i$) (C).

The second component finds the orthogonal directions in the X- and Y-spaces, which improves the description of these spaces as much as possible (Fig. 8A and 8B). These two lines form planes; scores t_1 and t_2 in X-space and u_1 and u_2 in Y-space. Equivalent with plot $u_1$versus t_1 (Fig. 7C), scores vectors t_2 and u_2 also indicate a correlative structure between X- and Y-spaces (Fig. 8C). As the first component explains most of the data variation, the correlation between t_2 and u_2 is weaker than the correlation between t_1 and u_1. Simultaneously, as the data variation is explained more completely, residuals become smaller. Additional components are treated with the same logic.

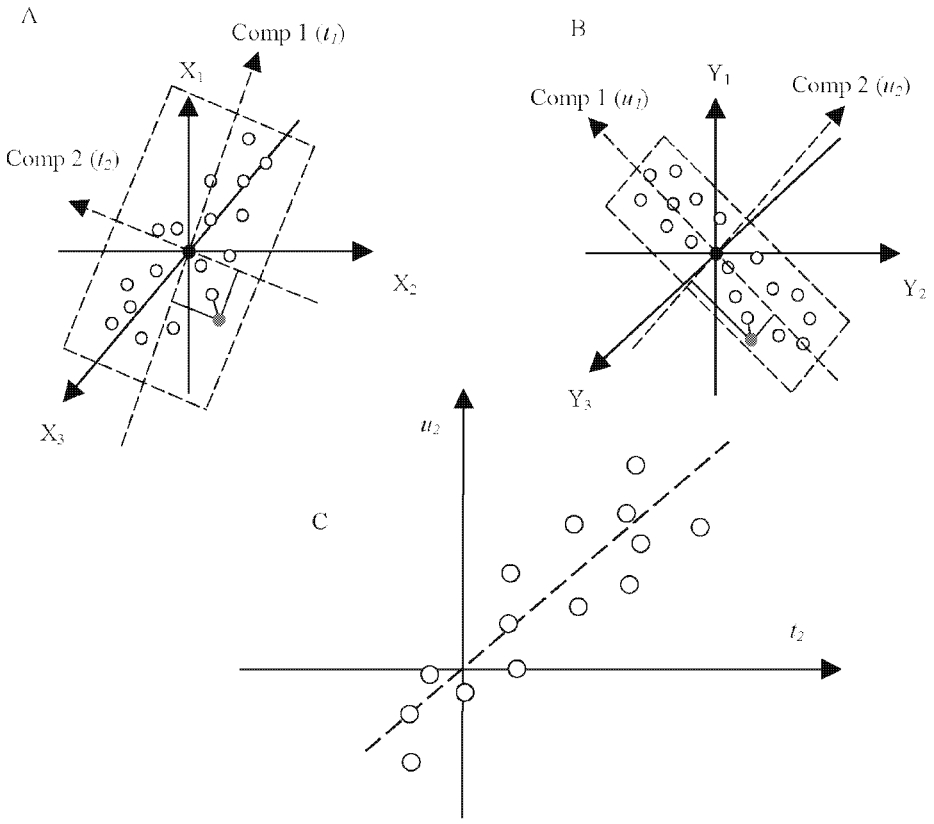

Figure 8. The second component is a line located orthogonal against the first component. First and second component lines form planes in the X- (A) and Y-spaces (B). Score vectors t_2 and u_2 (C) correlate weaker that the first pair of score vectors, which is found as a boarder point swarm compared to Fig. 7C.

The meaning of variables is given by weights, which is illustrated by the PLS loading plot in the same way as the PCA loadings (Fig. 9). The PLS weights describe the relationships among variables at the same time, and identifies which are associated and which contributed unique information. So, PLS tells what X gives Y and/or how to adjust X to get a desired Y. For example, as one increases the value of response variable A (Fig. 9), it has to increase the numerical values of X variables 1 and 2, as they are projected on the same side of the plot as response variable A, and/or decreases the numerical values of X variables 4 and 5, as they are projected on the other side of plot as response variable A. X variable 3 has no effect on response variable A, as it has been

projected on the plot origin. So, the decreasing magnitude of variables into the response is 5 > 4 > 1 > 2, which is actually the projecting length of variable from the plot origin.

PLS can also be used to predict unknown responses after a valid PLS model has been established. A new observation, which was not used in PLS model building, is located in the X-space (Fig. 10). Next, its projection on the X-model (t) is entered into the inner relation equation, which produces a u –value. This u –value defines a position on the Y-space model, which, in turn, corresponds to a predicted value for a response variable.

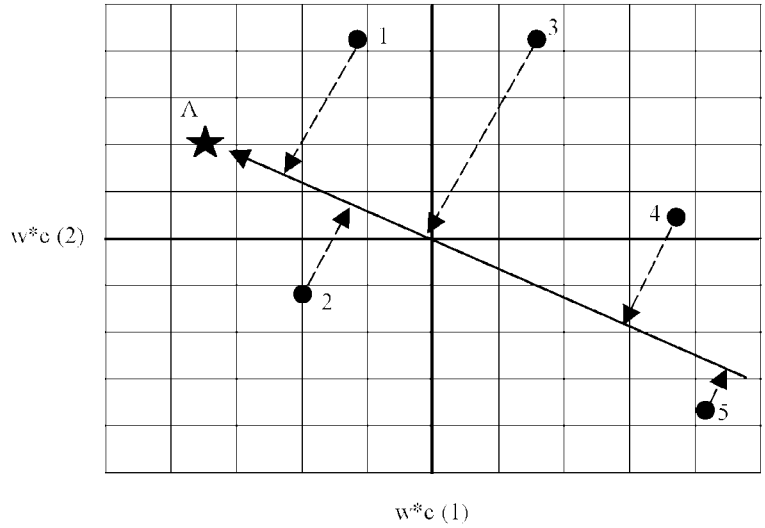

Figure 9. PLS weight plot, which tells the effect of X variables on Y responses.

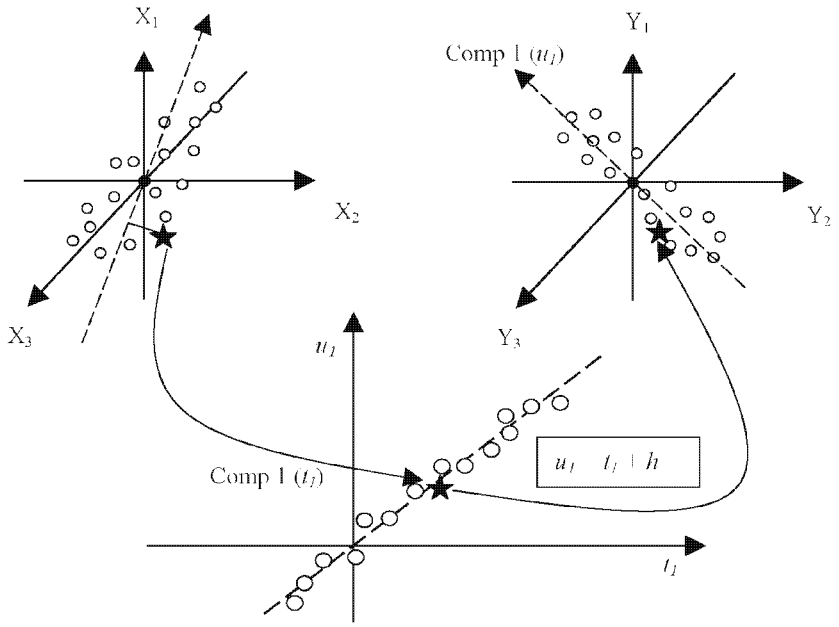

Figure 10. PLS prediction procedure. Open circles are observations used in model building and the star represents the predicted observation.

2.5 Pharmacokinetics

In vivo studies must be done in order to get a confirmation of whether or not a new agent is able to work as a release controlling excipient in humans. According to standardized procedures (EMEA 1999b), it should be demonstrated that the controlled release formulation has the claimed pharmacokinetic characteristics. Special interest is focused on the rate and extent of absorption, and fluctuation in the plasma concentration of a drug. The pharmocokinetic parameters of interest are peak plasma concentration (C_{max}), area under the curve (AUC), and the minimum plasma concentration in repeated dosing (C_{min}). AUC is determined by linear trapezoidal summation, C_{max} and C_{min} are obtained directly from the data.

The assessment of bioequivalency is based on a comparison of AUC and C_{max} between the test and reference product (FDA 1997a). To establish bioequivalency, the ratio of the geometric means of test and reference product and their 90% confidence interval of AUC and C_{max} should fall within the limits of 0.80-1.25.

2.5.1 *In vitro – in vivo* correlation (IVIVC)

Establishment of an IVIVC is very useful in guiding formulation and process development in the early stages (FDA 1997b). IVIVC can also facilitate scale-up, in addition to pre- and post-approval changes. FDA classifies IVIVC into four categories; A, B, C, and multiple C. Level A is a predictive mathematical model for the relationship between the entire *in vitro* release time course and entire *in vivo* response time course. A level A correlation is the most desired. Level B is a predictive mathematical model for the relationship between summary parameters that characterize the *in vitro* and *in vivo* time course; e.g., models that relate the *in vitro* MDT (mean *in vitro* dissolution time) to *in vivo* MDT (mean *in vivo* dissolution time) or *in vivo* MRT (mean *in vivo* residence time). Level C is a predictive mathematical model for the relationship between the amount dissolved *in vitro* at a particular time (e.g., Q_{60}), or the time required for the dissolution of a fixed amount (e.g.; $T_{50\%}$), and a summary parameter that characterizes the *in vivo* time course (e.g. C_{max} or AUC). Multiple level C is a predictive mathematical model for the relationship between the amount of drug dissolved at several time points for a product, and one or several pharmacokinetic parameters of interest.

IVIVC can be established if the dissolution rate is the rate-limiting step in drug absorption (Cardot and Beyssac 1993). According to the Biopharmaceuticals Classification System (BCS) (Amidon et al. 1995), IVIVC can be obviously established for drugs belonging to class I or II, if the release rate is controlled. Class I drugs are highly permeable in the intestine and highly soluble at physiological pH. With class II drugs, the permeability is high and solubility low.

2.5.2 Establishment of Level A IVIVC

The most commonly seen process for establishing a Level A IVIVC is to (1) develop formulations with different release rates (e.g.; fast, medium and slow), (2) obtain *in vitro* dissolution profiles and *in vivo* plasma concentration versus time profiles for these formulations and (3) estimate the cumulatice *in vivo* absorption profiles using an appropriate deconvolution technique for each formulation and subject (Fig. 11).

Different mathematical models have been used to correlate *in vitro* drug release and *in vivo* plasma concentrations of drug or the amount of drug absorbed (Loo and Riegelman 1968, Wagner 1983, Cutler 1978, Gillespie 1997). Convolution and

deconvolution methods form the basics in the establishment of Level A correlation (Qiu et al. 2000). The input function (*f(t)*) (i.e.; drug absorbtion in the GI-tract) can be obtained by using a convolution integral (Eq 6):

$$C(t) = f(t) \cdot C_{\delta}(t) \qquad (6)$$

where $C_{\delta}(t)$ is the unit impulse response (i.e.; plasma levels from an i.v. bolus) and $C(t)$ the impulse response (i.e.; plasma levels from oral solution).

The Wagner-Nelson and Loo-Riegelman model-dependent methods are commonly used for estimating *in vivo* drug absorption after oral administration of a drug (Qiu et al. 2000). Deconvolution methods are so-called "indirect" two-stage approaches, where *in vivo* drug absorption is determined by deconvolution and then compared to *in vitro* drug release. The Wagner-Nelson method is based on the mass balance, and the assumption of a one-compartment model. The advantage of the Wagner-Nelson method is that intravenous data is not necessary, but it utilizes the terminal phase elimination rate constant and AUC in determining *in vivo* drug absorption. The disadvantages are that only apparent absorption is estimated, and determination of the exact elimination rate constant is difficult, especially with extended drug release and/or long half-life of a drug.

Loo-Riegelman is another method for estimating the *in vivo* fraction absorbed. It copes with two- or more compartmental models (Loo-Riegelman 1968). The Loo-Riegelman method is also based on the mass balance between different compartments. In addition, this method requires intravenous data to determine rate constants between different compartments.

Some justified criticism has been directed towards deconvolution methods because of its indirectness (Gillespie 1997, O'Hara et al. 2001). The main disadvantages are the sensitivity or instability of deconvolution, and that it predicts the fraction of release and/or absorbed drug, rather than the plasma concentration of a drug. Method instability is due to the mathematics of the method, since the amount of time points for blood samples is often low, and thus, only a small change in the data can remarkably affect changes in response. However, after adequate damping or smoothening methods, it is possible to obtain reliable deconvolution methods (Proost 1985).

Convolution is an alternative method to establishing a Level A IVIVC. It can directly predict plasma concentrations using Equation 6 in a single step (Qiu et al. 2000). The basic assumption is a linear, time-invariant relationship between drug release and plasma concentration. The IVIVC is validated by comparing the predicted plasma

concentrations with the observed plasma concentrations. As in extended drug delivery, some drugs might be released beyond the site of drug absorption, which has been proposed as an extended convolution model (Gillespie 1997). This method utilizes cumulative amounts of released drug.

As the target of developing IVIVC is to establish a predictive model describing the relationship between *in vitro* characteristics and a significant *in vivo* response, the prediction performance must be validated. The internal predictability of a Level A correlation is based on the initial data set used to define the IVIVC. If one or more formulations do not reach acceptable limits then external predictability must be carried out based on an additional data set. Predictability is calculated as a prediction of percent error (*%PE*). The average of three predicted AUC and C_{max} measures should fall below a %PE of 10 % and the %PE for each formulation should not exceed 15%. External predictability is based on additional data set that is not used in the establishment of IVIVC, and from a scientific point of view, it might be beneficial carried out after the determination of internal predictability.

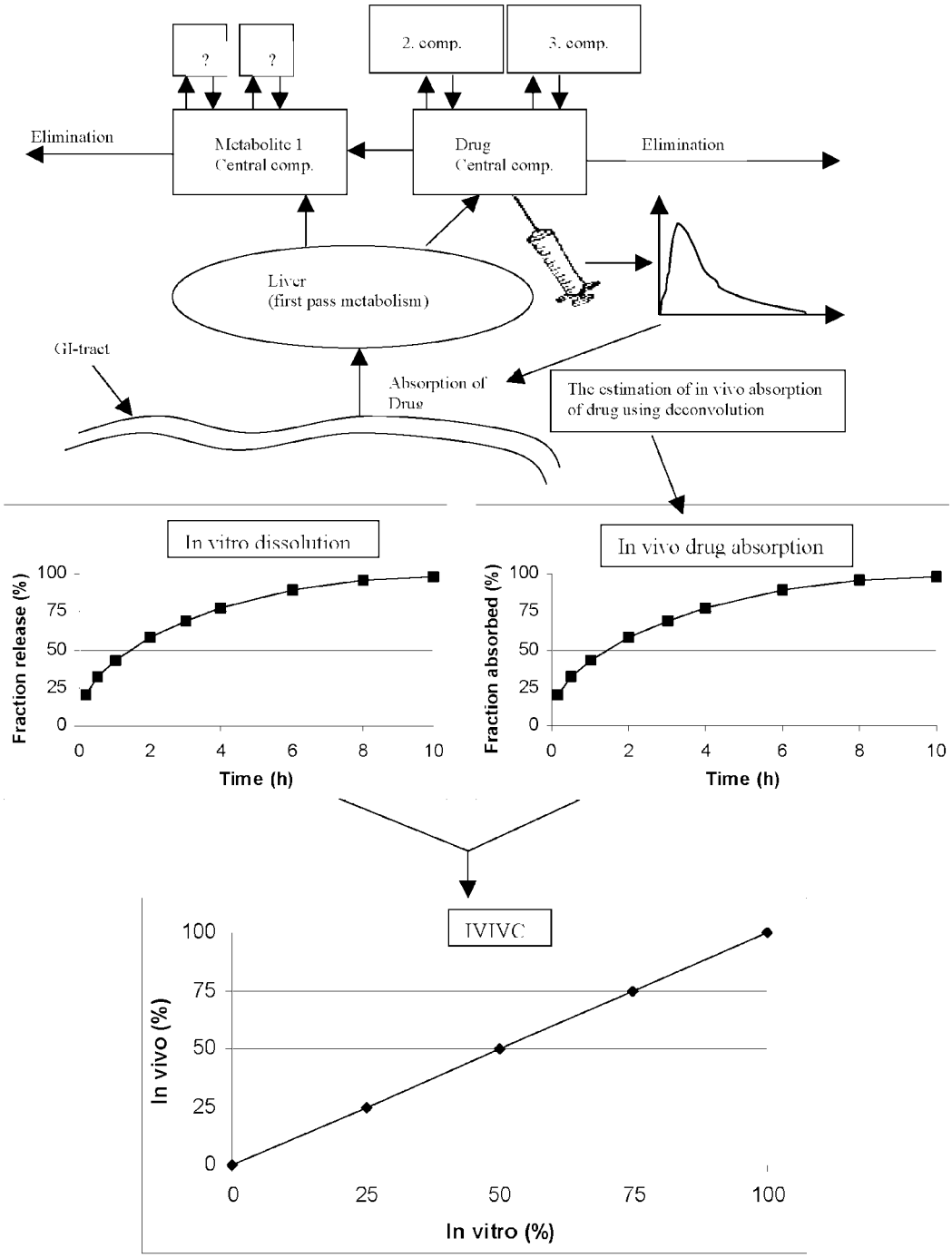

Figure 11. Schematic presentation of establishment of *in vitro – in vivo* correlation (IVIVC).

3 AIMS OF THE STUDY

The general objective of this study was to evaluate the applicability of starch acetate as a novel tablet excipient for oral extended drug release tablets. The specific aims were as follows:

1. To study the physicochemical, direct compressibility, tablet and drug release characteristics of starch acetates having different degrees of acetyl substitution.

2. To evaluate the impact of different drying methods on particle, powder, tableting and tablet properties of starch acetate (degree of substitution 2.6).

3. To determine factors affecting the release kinetics and mechanisms from tablets compressed from a binary mixture of different drug-starch acetate tablets using multivariate data analyses.

4. To evaluate the bioavailability of starch acetate - diltiazem tablets in human volunteers, and to confirm whether starch acetate acts as a drug release controlling excipient *in vivo*. To establish an *in vitro-in vivo* correlation using a direct cumulative area under the curve (AUCcum) approach.

4 EXPERIMENTAL

4.1 Materials

4.1.1 Starch acetate (I-IV)

All starch acetates **(I-IV)** were prepared by substituting a portion of the hydroxyl groups on a starch polymer with acetyl groups in an esterification reaction (VTT Rajamäki, Finland). Briefly, starch acetates were synthesized by allowing native starch to react with aceticanhydride in the presence of a 50% sodium hydroxide solution. The resulting mixture was cooled and the starch acetate was precipitated from water with vigorous mixing. The precipitate was filtered and washed thoroughly with water and dried. The degree of substitution of the starch acetate was adjusted by varying the amount of acetanhydride and base, and other reaction conditions.

Barley starch was used as a raw material in the preparation of starch acetate **(I)** having degrees of substitution (ds) of 0.34, 1.19, 2.10 and 2.90. A sieved fraction of 53-297 μm was collected and stored at 33 % relative humidity and room temperature prior to experiments.

In the preparation of starch acetate (ds 2.6) **(II)**, potato starch was used as a raw material. Starch acetate was used as received and stored at 33 % relative humidity and room temperature prior to experiments.

Also, in the preparation of starch acetate (ds 2.7) **(III, IV)**, potato starch was used as a raw material. A particle size fraction less than 500 μm was used and stored under the ambient conditions prior to experiments.

4.1.2 Reference direct compression excipients (I, II, IV)

The following direct compression excipients were obtained commercially; microcrystalline cellulose **(I, II)** (MCC) (Avicel™ PH101, FMC, USA) dicalcium phosphate dihydrate **(I, II)** (DCP) (Emcompress™, E. Mendell, USA) and modified starch **(I)** (MS) (Starch 1500™, Colorcon, England) and all were used as received and stored at 33 % relative humidity and room temperature prior to experiments. Magnesium stearate **(I, IV)** (0.5 % (w/w)) was used as a lubricant in tableting.

4.1.3 Model drugs (I, III, IV)

Anhydrous theophyllin **(III)**, diltiazem-HCl **(III, IV)**, ibuprofen **(III)** and propranolol-HCl **(I, III)** were obtained from Orion Pharma (Finland), and atenolol **(III)**, diclophenac-Na **(III)** was obtained from Leiras (Finland). All drugs fulfilled the quality requirements of Ph.Eur., and were used as supplied.

4.1.4 Other chemicals (I, III, IV)

Chemicals for the preparation of dissolution mediums and liquids for chromatography were obtained from commercial suppliers and used as received. All materials were at least of analytical grade and, in the case of liquids for chromatography, chromatographic grade.

4.2 Methods

4.2.1 Drying procedure of starch acetate (II)

Starch acetate **(II)** was synthesized up to drying phase as described above, and the resulting starch acetate slurry was dried by four different dryers: batch 1 (Lödige VT50, Gerb Lödige Maschinenbau GmgH, Paderporn, Germany); batch 2 (Drais Turbudry TD20, Draiswerke GmbH, Speckweg, Germany); batch 3 (Anhydro tunnel-shaped fluid-bed dryer, APV Anhydro AS, Copenhagen, Denmark); and batch 4 (Laboratory Spin Flash dryer, APV Anhydro AS, Copenhagen, Denmark) (Table 1). Dryers for batches 1 and 2 were horizontal vacuum rotary dryers (conduction) (Moore 1987). The dryer for batch 3 was a fluid bed dryer (convection). The dryer for batch 4 was a mechanical agitated fluid bed dryer (convection), or "spin flash" dryer. This fourth dryer was similar to the fluid bed dryer, but contained an additional mechanical agitator.

Table 1. Dryers and Drying Parameters*

Drying Method	Drying Temp (°C)	Vacuum (mbar)	Batch Size (kg)	Yield (%)	Drying Time (min)	Residual Moisture (%)	Batch Code
Lödige VT50	70†	100	6.3	66	120	6	Batch 1
Drais Turbudry TD20	45-92‡	45-170	70	81	90	1	Batch 2
Anhydro tunnel-shaped fluid-bed dryer	140§	-	nd	nd	240	5	Batch 3
Laboratory spin flash dryer	140§	-	12	89	75	5	Batch 4

*nd indicates not determined.
†Jacket temperature.
‡Material temperature during drying.
§Air inlet temperature (outlet temperature was 70 °C in batch 4, but outlet temperature of batch 3 was not known).

4.2.1 Characterization of starch acetate (I)

Determining of the substitution degree of starch acetates was done as described in the literature (Wurzburg 1964).

4.2.2.1 Differential scanning calorimetry (DSC) (I)

Differential scanning calorimetry (DSC) (Perkin-Elmer DSC7, Perkin-Elmer Co., USA) was used in the determination of glass transition temperatures (Tg) for starch acetate. Samples (4-6 mg) were closed in 50µl aluminum pans with holes. The heating program was as follows; heating from 20 °C to 200 °C (20 °C/min); cooling to 100 °C (20 °C/min) and a second heating up to 200 °C (10 °C/min), where the glass transition temperatures were determined and expressed as a mean of three parallel scans.

4.2.2.2 X-ray powder diffractometry (I)

Crystal structures were determined by using X-ray powder diffraction. Diffraction patterns were obtained by a Philips PW1710 automated powder diffractometer system (Philips, The Netherlands) with the following conditions; Cu tube anode as a source of radiation (wavelength = 0.15456 Å), voltage 50 kV, current 40 mA, automatic divergence slit (irradiated sample length 12 mm), receiving slit 0.2 mm a proportional detector step size of 0.025°, sample time 1.00 s, and a peak angle range of 1.000-

40.000°. Data were collected and analyzed using the Philips ADP1700 software program.

4.2.3 Particle and powder properties (I, II, III)

The particle size **(I)** of starch acetate sample was calculated from digitized images of the scannig electron micrographs (SEM) (Jeol JSM-35, Japan). Also, scanning electron microscopy was used in the visual evaluation of surface texture **(II)** of the starch acetates. The Martin's diameter was measured from at least 740 starch acetate particles and at least 400 reference material particles.

The particle size **(II)** and size distribution **(II)** of the powder was determined by a laser diffractometer (Malvern Instruments Ltd, Mastersizer 2000, Worcestershire, England) by the particle in liquid (ethanol) method. Particle agglomerates were decomposed using ultrasound. The use of ultrasound was terminated when particle size did not change between individual measurements. Next, particle size was determined as the mean of 10 measurements. Results are expressed as $D(v, 0.1)$, $D(v, 0.5)$, and $D(v, 0.9)$, where $D(v, 0.1)$, $D(v, 0.5)$, and $D(v, 0.9)$ are particle sizes (D) in microns at 10%, 50%, and 90% of the sample size, respectively. The term "v" indicates that particle size determination was based on the volume of a sphere that is equivalent to the measured particle. Particle size distribution was determined as a span, measured as the width of the size distribution; i.e.; the narrower the distribution, the smaller the span becomes. The span was calculated from Equation 7.

$$Span = \frac{[(D(v,0.9) - D(v,0.1))]}{D(v,0.5)} \qquad (7)$$

Particle densities **(I, II, III)** (Ph Eur 2.2.24) of the powders were measured with a multipycnometer (Quanta Chrome, Syosset, NY, USA) using helium as a measuring gas. Bulk density **(II)** was determined by carefully pouring the powder into a glass cylinder, then calculating the mass of powder by dividing it with the powder volume. For tap density **(II)**, the cylinder was tapped for 10 minutes (Erweka SVM, Erweka Apparatebau GmbH, Heusenstamm, Germany). The tap density was calculated as the bulk density, as describe above. Densities were determined as the mean of five measurements.

The volume reduction **(II)** of a powder due to tapping was calculated by the Kawakita equation (Eq. 8) (Ludde and Kawakita 1966):

$$\frac{N}{C} = \frac{N}{a} + \frac{1}{ab} \tag{8}$$

where N is the number of taps, and both a and b are constants. The constants of the Kawakita equation can be used to estimate the flow and cohesive properties of powders. Constant a describes the compressibility and constant $1/b$ describes cohesive properties of a powder, or the amount of time it takes to achieve the final packing stage. Term C describes volume reduction during the tapping treatment, and was calculated by Equation 9:

$$C = \frac{(V_0 - V_N)}{V_0} \tag{9}$$

where V_0 is the loose volume of the powder column before tapping, and V_N is the volume of the powder column after a certain number of taps (N).

Flowability **(I)** of the samples was determined using the standard Ph.Eur. (2.9.16) method. Briefly, forty grams of powder mass, which contained 99.5% (w/w) of the excipient and 0.5% (w/w) of magnesium stearate as a lubricant, were placed in a funnel and allowed to flow. The orifice of the funnel was fixed 6 cm above the base. Flowing time **(I)** was measured and results were presented as seconds per 100 g of powder mass. The angle of repose **(I)** was calculated from the formed powder pile by equation 10,

$$\tan\theta = \frac{h_e}{r} \tag{10}$$

where h_e is height of the pile of powder and r is the radius of the base at the cone. Results are expressed as a mean of three determinations. In the case of same experiments **(II),** the angle of repose was determined from a twenty gram powder sample and results are the expressed as the mean of five determinations.

The water content **(I)** of powders was measured using a Karl-Fischer titrator (Mettler DL 35 Karl-Fischer titrimeter, Switzerland). Results are the means of five determinations. Powder samples were stored at 33% relative humidity and room temperature at least seven days before measurements. Residual water **(II)** after different drying methods was measured gravimetrically. Water content **(II)** of the powders was measured by the gravimetric method. Powders were stabilized at 33% relative humidity at room temperature prior to measurements. Stabilized powder samples were placed in

petri dishes and dried in the oven at +170 °C (Termaks, Norway). The weight loss was obtained by accurately weighing the sample after 24 hours of drying. Results are expressed as the mean of three parallel determinations.

The specific surface area **(II)** (SSA) of powdered samples was determined by the single-point BET method (Micromeritics, Flowsorb II 2300, Norgross, GA, USA). A nitrogen/helium (70%/30%) gas mixture was used as a measuring gas. Powders were dried under vacuum and +40 °C for 24 hours before determination. Results are expressed as the mean of five determinations.

4.2.4 Tableting (I-IV)

Tablets **(I)** contained 0.5 %(w/w) magnesium stearate as a lubricant and were compressed with an instrumented eccentric tablet press (Korsch EK-0, Germany) at a press speed of 30 rpm using flat faced punches and a die of 10 mm in diameter. Compression pressures of 90, 190 and 320 MPa were used. Tablet weights were adjusted to give a theoretical thickness of 1.5 mm at zero porosity, taking into account the diameter of the die and the particle densities of the excipients. Scanning electron micrographs (Jeol JSM-35, Japan) were taken after compression to examine the surface structure of the tablets **(I)**.

Tablets **(II)** were compressed with a compaction simulator (PCS-1, PuuMan Ltd, Finland) using a 10-mm diameter flat-faced punch and die set. A compression pressure of 200 MPa was applied at rate of 30 mm/s. The upper punch followed a saw-tooth profile, while the lower punch was kept stationary during compression. The weight of tablets was adjusted to give a theoretical thickness of 1.5 mm at zero porosity, taking into account the diameter of the die and the particle density of the material. Force-displacement data were collected from 4 parallel compressions and corrected according to punch deformations.

A two level, three-factor experimental design with a centre point was used to produce tablets **(III)** with different drugs. Porosity of the tablet, drug/starch acetate ratio and tablet mass were used as determining factors. The formulations of the starch acetate tablets for evaluating drug release properties are presented in Table 2. For each formulation, accurately weighed amounts of drug and starch acetate were thoroughly mixed in a mortar. The mixture was then compressed using a compaction simulator (PCS-1, Puuman Ltd, Finland) with 10 mm diameter flat-faced punches. A double sided-sine wave compression profile was used. The height and duration of the profile

was 6000 μm and 400 ms, respectively. The simulator was adjusted to produce the desired tablet porosity by taking into account the material densities, powder masses and diameters of the tablets. Three tablets of minimum weight and porosity deviation from the respective theoretical values were selected for the dissolution studies.

Three different starch acetate – diltiazem tablets **(IV)** were formulated to produce fast, equal and slow drug release profiles, compared to a reference product. Formulations contained 50% (fast), 35% (intermediate) and 15% (slow) diltiazem, designated as D15, D35 and D50, respectively. Each formulation contained a total of 90 mg of diltiazem and 0.5 m/m% of magnesium stearate as a lubricant.

Table 2. Formulations (A-I) and process factors studied.

Component	A	B	C	D	E	F	G	H	I
Drug (%w/w)	5	5	5	5	10	15	15	15	15
Starch acetate (%w/w)	95	95	95	95	90	85	85	85	85
Tablet porosity (%)	5	10	5	10	7.5	5	10	5	10
Tablet mass (mg)	200	200	250	250	225	200	200	250	250

4.2.4.1 Volume reduction, forces and works during tableting (II, III)

Volume reduction properties of the powders **(II, III)** were evaluated from force-displacement data using the Heckel equation (Eq. 11) (Heckel 1961 a and b):

$$\ln\left[\frac{1}{(1-D_p)}\right] = (k_s \cdot P) + A \qquad (11)$$

where D_p is the relative density of a powder column at compression pressure P. The reciprocal of slope (k_s) from the Heckel plot is referred to as the yield pressure (P_y). Constant A in the Heckel equation is related to the die filling and particle rearrangement phases before deformation and particle bonding. The relative densities of the powder beds at the very beginning of compression were calculated by Equation 12:

$$D_A = D_0 + D_b \qquad (12)$$

where D_0 describes the relative density due to die filling, D_b represents the particle rearrangement phase, and D_A includes both the die filling and particle rearrangement phases.

The following compaction properties **(III)** were determined; the maximum compression force of the upper (F_{up}) and lower (F_{lo}) punches, maximum ejection force (F_{ej}), minimum tablet height (H_{min}) during compression, absolute and relative work of the upper (W_{up}) and lower (W_{lo} and W_{rlo}) punches, absolute and relative works of expansion (W_{exp} and W_{rexp}), friction (W_{fri} and W_{rfri}), ejection (W_{ej} and W_{rej}) and net work (W_{net} and W_{rnet}) (De Blaye and Polderman 1970, 1971, Ragnarsson and Sjogren 1983, 1985).

4.2.5.2 Characteristics of tablets (I, II, III,)

Breaking strength, height and diameter of tablets **(I, II)** were measured 24 hours after tableting. Breaking strengths were measured with an universal tester (CT-5 tester, Engineering Systems, England) operated at a constant cross head speed of 1 mm/min. The tensile strength of tablets was calculated according to Fell and Newton (1970) (Eq. 13):

$$\sigma = \frac{2 \cdot F}{\pi \cdot h_e \cdot d} \tag{13}$$

were F is the breaking force, h_e is the tablet height, and d is the tablet diameter.

The friability **(I)** (Ph.Eur. 2.9.7) was determined from tablets at compression pressures of 90, 190 and 320 MPa. Six tablets were placed in a Roche friabilator (Erweka, Germany) for four minutes at 25 rpm. The loss of tablet weight was calculated as a percentage of the initial weight.

Disintegration studies **(I)** were made according to the specifications of the Ph. Eur. (2.9.1) method with discs (Erweka, Germany). The disintegration medium was distilled water (800 ml) maintained at 37 ± 1.0 °C.

The weight, and dimensions of tablets were measured at least 24 hours after tableting. The density (ρ_m) of the tablet **(III)** was calculated according to Equation 14:

$$\rho_m = \frac{m}{\pi \cdot r^2 \cdot h_e} \tag{14}$$

where m is the weight of the tablet, r is the radius and h is the height. Porosity (ε) of the tablet **(I, II, III)** was calculated according to Equation 15:

$$\varepsilon = \left[1 - \left(\frac{m}{V} \right) \frac{}{\rho_m} \right] \cdot 100\% \qquad (15)$$

where m is the weight of the tablet, V the volume and ρ_m the particle density. Elastic recovery (ER%) of the tablet **(II, III)** was calculated according to Equation 16:

$$ER\% = \left[\frac{(H_{24} - H_{\min})}{H_{\min}} \right] \cdot 100\% \qquad (16)$$

where H_{min} is the height of the tablet at the maximum compression pressure and H_{24} is the tablet height at 24 hours after compression.

4.2.5 *In vitro* drug dissolution (I, III, IV)

Drug release from tablets was determined by the USP dissolution test method (USP XXIV) with basket **(I, III)** and paddle **(IV)** at 900 rpm (Sotax AT6, Switzerland). The volume of dissolution medium was 900 ml, maintained at 37 ± 0.5 °C. Detailed dissolution medium compositions and sampling times are given in the original papers **(I, III, IV).**

4.2.5.1 HPLC-chromatography for *in vitro* drug dissolution (III, IV)

Drug analysis was performed by a Gilson HPLC system consisting of a 234 autoinjector (Gilson, France), 321 pump (Gilson, France), UV/VIS-151 detector (Gilson, USA), system interface module (Gilson, USA) and Unipoint™ LC system version 3.01 software (Gilson, USA). A loop injection volume of 20µl and flow-rate of 1 ml/min were used. The analytical column was Inertsil® ODS-3 (4.0mm x 150mm) (Japan). The column was kept at +40 °C with a column oven (Crocosil, France). The mobile phases and wavelengths are shown in Table 3.

Table 3. HPLC assay for the analysis of dissolved drug.

Drug	Amount of AcN[a] (%)	Amount of Water (%)	Amount of TFA[b] (%)	Wave-length (nm)
Propranolol HCl	30	70	0.03	289
Atenolol	10	90	0.03	274
Verapamil HCl	35	65	0.03	229
Diltiazem HCl	30	70	0.03	237
Ibuprofen	70	30	0.10	214
Diclofenac Na	65	35	0.10	237
Theophylline anhdr.	10	90	0.03	271

AcN[a] = Acetonitrile, HPLC-grade (Rathburn, UK)
TFA[b] = Trifluoroacetic acid, spectrophotometric grade (Aldrich, USA)

4.2.5.2 Analysis of drug release kinetics and rates (I, III, IV)

Power Law equation was used to evaluate drug release from the starch acetate matrix in **I, III** and **IV** papers. The dissolution data was fitted according to the Power Law equation (Eq. 17) (Korsmayer et al., 1983):

$$\frac{M_t}{M_\infty} = k \cdot t^n \qquad (17)$$

where M_t/M_∞ is the fractional (0-0.6 (**I, III**) and 0-0.75 (**IV**)) drug release at time t, k is a constant incorporating the matrix structure, and n is a diffusional exponent, which was used to characterized the transport mechanism. When n was 0.43-0.50, the release mechanism indicated a pure diffusional release of the drug (time squared release kinetics), and when n was 1.00, drug release followed zero-order transport (constant drug release) (Ritger and Peppas 1987). Values between 0.50 and 1.00 indicated an anomalous release of the drug.

4.2.5.3 Multivariate analysis of drug release mechanisms and kinetics (III)

A Principal Component Analysis (PCA) was used to summarize data contained in the X-matrix; indicating strong outliers and main influential variables, using SIMCA-P (Version 10.0, Umetrics, Sweden) software. Data was pre-treated by unit variance scaling and mean centering for normalizing the weight of each variable in the model. Eight main components (PC) were used to describe the data matrix. The PCA score plot

t[1]/ t[2] and *Hotelling's* T^2 diagnosis at the 95% confidence level were used to observe strong outliers.

PLS was used as a regression extension of PCA (SIMCA-P, Version 10.0, Umetrics, Sweden). In the PLS, a quantitative regression between the variables and observations was determined. Diffusional exponent (n) and drug release rates (k) were studied separately. As explanatory variables (n=52), different formulations, compressions, tablet and drug properties were used (original paper **III**, Table 3). Data was pre-treated using a unit variance scaling and mean centering for normalizing the weight of each variable in the model. Also, skewed variable distributions were normalized by Log or power transformations. Strong outliers were determined by *Hotelling's* T^2 diagnosis at the 95% confidence level. Insignificant variables were detected by variable influence on projection (VIP). Variable having the lowest VIP value were excluded from the model and, that variable was permanently removed, if the value of the prediction parameter (Q^2) subsequently increased. This procedure was repeated until the Q^2 parameter did not improve any more.

4.2.6 Bioavailability (IV)

An open, single dose, randomised, 4-treatment, 4 period, 4 sequence, cross-over trial was conducted in eight healthy volunteers, to evaluate plasma concentration-time curves of the three formulations and the reference product (Dilzem 90mg depottabl, Orion Pharma, Finland). Each treatment period followed a two-week wash out period to eliminate the effect of each tested dose before the next treatment. C_{max} was directly recorded from plasma concentration-time profiles and the $AUC_{0-\infty}$ was calculated according to the trapezoidal rule by using the WinNonlin Professional software package (version 4.0.1, Pharsight, USA) for pharmacokinetic calculations.

4.2.6.1 Validated assay of diltiazem plasma samples (IV)

The following international guidelines and requirements were followed in the present study; Validation of Analytical Methods, Definitions and Terminology, ICH Topic Q2A and Validation of Analytical Procedures and Methodology, ICH Topic Q2B, including specificity, limit of detection and quantification, linearity, precision and accuracy, intra- and inter-day variability, stability in the freezer and autosampler. Plasma samples were frozen at –20 °C at the clinical study site immediately after separation of the plasma.

Plasma was prepared for analyses by extraction with acetonitrile. The same procedure was used for the preparation of samples for the calibration curve construction, quality control samples and samples from the clinical trial. Plasma samples were thawed at room temperature. 700 µl of plasma was transferred to 2.2 ml vial. To this plasma sample, 50 µl of 7 µg/ml verapamil (internal standard) solution was added and vortex-mixed for 10 seconds. Then 900 µl of acetonitrile was added and the sample was vortex-mixed for 1 minute. The resulting sample was centrifuged at 6400 rpm for 10 min at 10 °C. Vials were kept frozen overnight at –20 °C. Freezing of the samples allowed efficient separation of aqueous and organic phases. From frozen samples 600 ml of the organic phase was removed with a pipette and transferred to a 1.5 ml vial. The solvent was evaporated to dryness under a stream of air. The sample was reconstituted in 120 µl of mobile phase, vortex-mixed for 0.5 minute and centrifuged at 6400 rpm for 10 min at 10 °C. 70 µl of this solution was transferred to the auto sampler vial. The previously validated chromatographic conditions were as follows; column: Lichrosorb RP-18, i.d. 5 µm, 250x3.2 mm (Alltech Associates Inc., USA), loop injection volume 40 µl, mobile phase acetonitrile 0.01 M phosphate solution (Na_2HPO_4), triethylamine 15:85:1, flow rate 0.7 ml/min, detector wavelength 237 nm, column temperature 21–23 °C (room temperature), temperature in autosampler 10°C, run time 13 min.

4.2.6.2 Establishment of *In Vitro – In Vivo* correlation and Bioequivalency (IV)

The cumulative $AUC_{0\text{-}24h}$ of time profiles (*AUCcum(t)*) was generated from averaged concentration-time profiles of diltiazem in plasma without further time scaling. *AUCcum(t)* of each formulation was fitted to the Hill equation and constants *a*, *b* and *c* were determined (Eq. 18) (Balan et al. 2001):

$$AUCcum(t) = \frac{a \cdot t^b}{c^b + t^b} \qquad (18)$$

where *a*, *b* and *c* are constants, and *AUCcum(t)* is the cumulative area under curve at time *t*. Average profiles of *in vitro* dissolution were fitted by Power Law equation 16 up to 75%. Next, a correlation analysis was conducted to find correlations between Hill's constants and *in vitro* drug release rates and diffusional exponents. Finally, the predicted *AUCcum(t)* was calculated from the *in vitro-in vivo* regression equation and Hill function. The internal predictability of IVIVC was evaluated to ensure the predictive performance of the model, using a percent prediction error (%PE)

calculation. Predicted $AUC_{0\text{-}24h}$ and C_{max} were compared to the observed $AUC_{0\text{-}24h}$ and C_{max} using equation 19:

$$\%PE = \left[\frac{(Obs - \Pr ed)}{Obs}\right] \cdot 100\% \qquad (19)$$

Bioequivalence was determined according to FDA guidelines (2001) using the WinNonlin software package (version 4.0.1, Pharsight, USA). The bioequivalency was based on a comparison of $AUC_{0\text{-}\infty}$ and C_{max}, between the test and reference products. The bioequivalency was calculated at the of 90% confidence level for the ratio of the geometric means of the measures for the test and reference products.

5 RESULTS AND DISCUSSION

In this study, a set of pharmaceutical and biopharmaceutical studies were carried out to evaluate the applicability of starch acetate as a novel excipient for extended oral drug delivery.

5.1 Characterization of starch acetate (I, II, III, IV)

The synthesis of starch acetate produced a ds of 0.34, 1.19, 2.1 and 2.9 for barley starch acetates **(I)** and a ds of 2.6 **(II)** and 2.7 **(III, IV)** for potato starch acetate.

In thermal analysis, the DSC thermograms **(I)** of the first heating cycle showed a broad endothermic dehydration peak between 30 - 190 °C for starch acetates having a ds of 0.34, 1.19, 2.1 and 2.9, with corresponding enthalpy changes of 251 ± 10.6, 158 ± 1.0, 69 ± 6.2 and 35 ± 1.2 J/g, respectively. The glass transition temperatures of starch acetates with ds values of 0.34, 1.19, 2.1 and 2.9 obtained from the second heating cycle were 159, 159, 166 and 156 °C, respectively. This means that T_g is not affected by the degree of acetylation of starch acetate.

X-ray powder diffraction patterns **(I)** demonstrated that starch acetates of ds 1.19, ds 2.1 and ds 2.9 exist in a totally amorphous molecular structure. The diffraction pattern of starch acetate ds 0.34 had some small reflections, which indicates that the molecular structure of ds 0.34 include some highly ordered crystalline regions, though it is mostly amorphous. Thus, upon increasing acetylation the molecular structure remained in as an amorphous form.

5.2 Physicochemical properties of starch acetate powders (I, II)

Particle sizes of starch acetate of different ds **(I)** were quite small and eqvivalent between different ds values, and similar to microcrystalline cellulose (MCC) and modified starch (MS), according to Martin's diameter (Table 4). The starch acetate particle shape became slightly more irregular as the ds increased (Fig. 12).

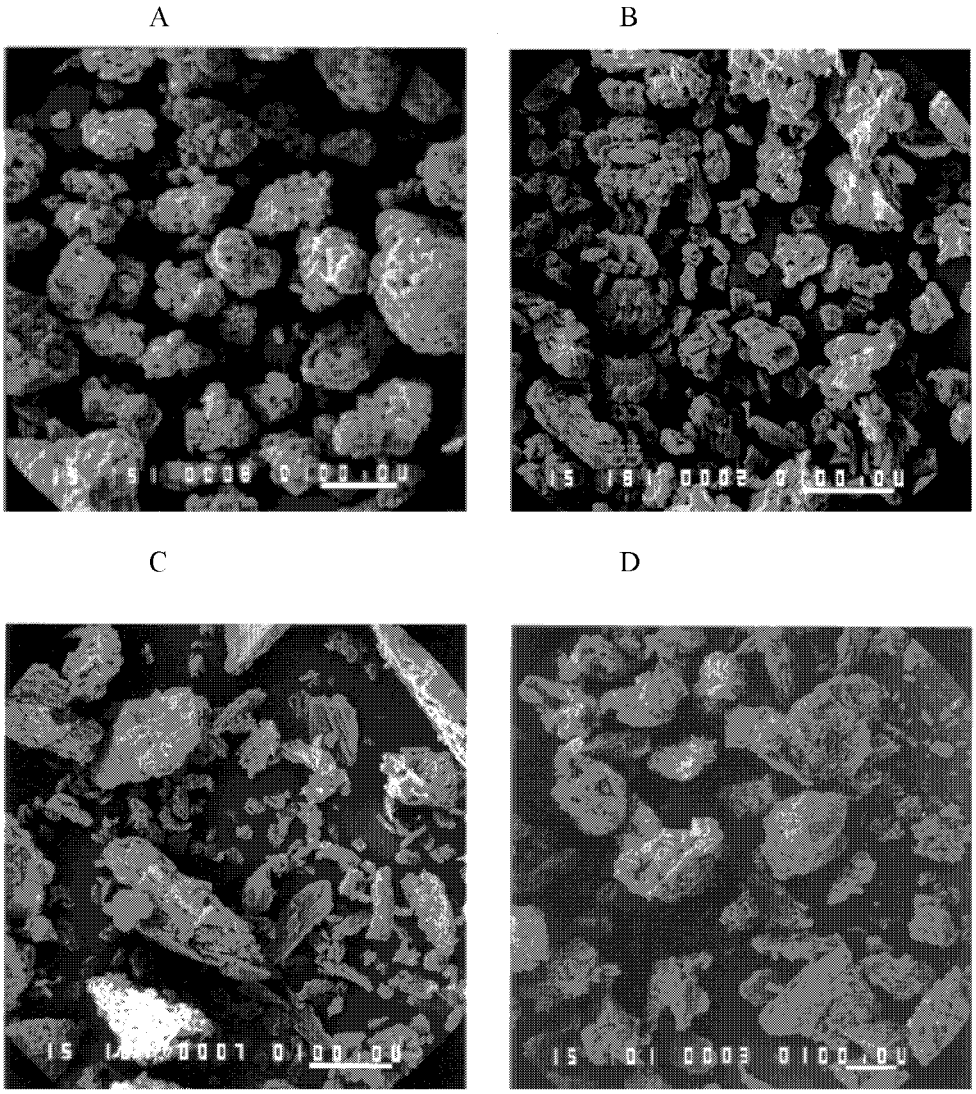

Figure 12. Micrographs of starch acetate powders having different degrees of substitution (ds) 0.34 (A), 1.19 (B), 2.1 (C) and 2.9 (D). The reference bar is 100 μm.

Table 4. Powder properties of starch acetates having different degrees of substitution (ds) and some common used tableting excipients*.

	Particle density (g/cm^3)	Martin´s diameter (μm)	Flowability (sec/100g)	Angle of repose (degree)	Water content (%)
starch acetate ds 0.34	1.515	49	4	21	7.5
	(0.001)	(47)	(1)	(1)	(<0.1)
starch acetate ds 1.19	1.461	32	6	22	5.1
	(0.005)	(21)	(1)	(1)	(<0.1)
starch acetate ds 2.1	1.347	55	5	25	2.3
	(0.005)	(38)	(<1)	(<1)	(<0.1)
starch acetate ds 2.9	1.367	69	8	23	1.5
	(0.005)	(55)	(<1)	(1)	(<0.1)
microcrystalline	1.656	30	X	X	5.0
cellulose	(0.003)	(22)			(0.1)
dicalcium phosphate	2.332	163	3	16	0.7
dihydrate	(0.001)	(67)	(<1)	(<1)	(0.2)
modified starch	1.527	30	3	21	8.0
	(0.003)	(27)	(1)	(1)	(1.4)

X = microcrystalline cellulose that did not flow through the funnel.
*SDs presented in parentheses.

Particle size and shape properties of starch acetates can be modified by optimizing the precipitation and drying conditions during the manufacturing process **(II)**. In the case of batch 1, a relatively low drying temperature and moderate vacuum induced a slow removal of water, which resulted in large spherical particles having a smooth surface and wide particle size distribution (Table 5, Fig. 13 and 14). The almost total absence of small particles might be due to the vacuum filter, which may have allowed small particles to pass through.

Batch 2 was also dried at a relatively low temperature, but a more effective vacuum and more powerful agitation resulted in a more efficient removal of water (residual moisture 1 %) than with batch 1. Due to the fast drying and powerful agitation, the particles of batch 2 were smaller, more irregular, but had a quite smooth surface compared to batch 1. Also, the specific surface area was larger for batch 2 and particle size distribution was narrower than for particles from batch 1 (Table 5, Fig. 14).

The drying of batches 3 and 4 was based on the fluid-bed method. Vigorous mixing of the fluidized particles and excellent heat transfer properties between the solid and gas phases led to the rapid evaporation of water. This method produced small, irregular, and porous particles having a large specific surface area. The particle size distribution of batches 3 and 4 were narrower than that of batches 1 and 2 (Table 5, Fig. 14).

Water content of starch acetate powders (**I**) changed as a function of acetate content (Table 4), which was also seen in the thermal analysis earlier. The water content decreased as the ds increased. The water content % (w/w) of starch acetates ds 0.34 (7.5%) and 1.19 (5.1%) powders was at similar to MS and MCC, respectively. Furthermore, water contents after different drying methods (**II**) were almost equal (Table 5).

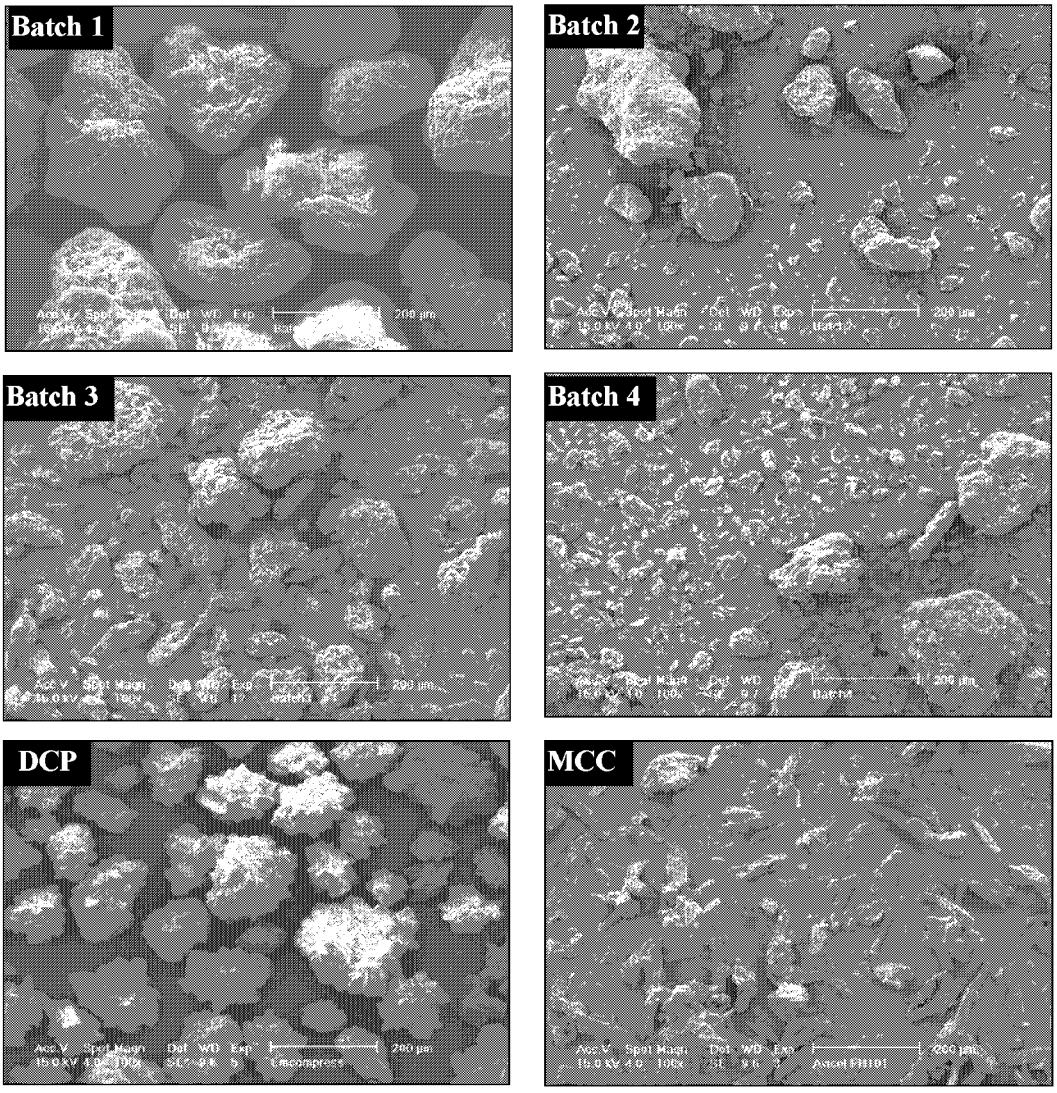

Figure 13. Scanning electron micrographs from powders. The reference bar is 200 µm.

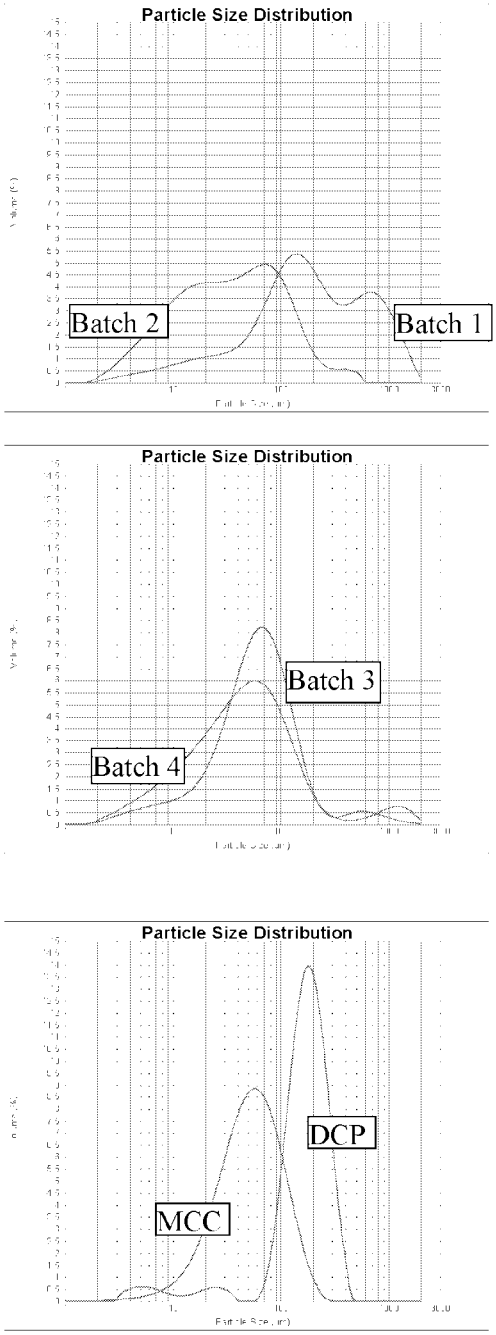

Figure 14. Particle size distributions of differently dried starch acetate and reference powders.

Table 5. Material Properties after different drying methods*

Drying Method	Particle Density (g/cm^3)	Particle Size D(v, 0.1) (μm)	Particle Size D(v, 0.5) (μm)	Particle Size D(v, 0.9) (μm)	Particle Size Distribution (Span)	Specific Surface Area (m^2/g)	Water Content (%)
Batch 1	1.36 (0.01)	24 (1)	165 (9)	851 (97)	5.0	4.84 (0.02)	2.0 (0.1)
Batch 2	1.37 (<0.01)	7 (<1)	34 (1)	132 (4)	3.7	6.71 (0.07)	1.3 (0.1)
Batch 3	1.38 (0.01)	16 (<1)	60 (1)	159 (22)	2.4	9.32 (0.33)	1.8 (0.1)
Batch 4	1.37 (0.01)	9 (<1)	45 (1)	164 (22)	3.4	10.46 (0.09)	2.2 (0.1)
MCC	1.66 (<0.01)	20 (<1)	53 (<1)	118 (<1)	1.8	1.01 (0.01)	4.4 (0.2)
DCP	2.33 (<0.01)	88 (1)	172 (1)	288 (2)	1.2	0.67 (<0.01)	0.2 (0.1)

*SDs presented in parentheses.

5.3 Bulk properties of starch acetate (I, II)

The particle density **(I)** of starch acetates decreased as ds increased, but the drying method did not seem to affect the particle density **(II)** of starch acetate (Table 4 and 5). The bulk and tap densities **(II)** of starch acetate ds 2.6 from different drying methods were essentially the same as with the reference product MCC, excluding batch 2, where bulk and tap densities were considerably higher. Batch 2 had the smallest particle size, with moderately large particle size distribution, which might have promoted the dense bulk and tap states of the powder. Obviously, the particle size was not too small, which would have caused cohesive problems.

Table 6. Powder Properties*

Drying Method	Bulk Density (g/cm^3)	Tapped Density (g/cm^3)	Angle of Repose (°)	Kawakita Compressibility (a)	Kawakita Cohesiveness (1/b)
Batch 1	0.34 (<0.01)	0.39 (<0.01)	17 (1.5)	0.15 (0.01)	23 (7)
Batch 2	0.44 (<0.01)	0.56 (0.01)	23 (1.3)	0.22 (0.02)	18 (2)
Batch 3	0.32 (<0.01)	0.39 (<0.01)	20 (0.5)	0.19 (0.01)	11 (1)
Batch 4	0.29 (<0.01)	0.40 (0.01)	24 (2.0)	0.28 (0.01)	15 (2)
MCC	0.29 (<0.01)	0.42 (<0.01)	X	0.31 (0.01)	23 (2)
DCP	0.83 (0.01)	0.92 (0.02)	15 (3.6)	0.16 (0.02)	50 (12)

*SDs presented in parentheses.
X indicates that MCC did not flow through the funnel.

Kawakita constants indicated the behavior of powder densification from the bulk density state to the tap density state (Table 6). Batch 1 densified the least (i.e., the smallest compressibility value) and attained the final packing state most slowly (i.e., the greatest cohesive value). On the other hand, batch 4 densified considerably but achieved

the final packing state rather quickly. The high 1/*b*-value for DCP could be due to the slow fragmentation of DCP and rearrangement of these new fragments during tap treatment.

Although some starch acetates exhibited relatively small particle size, they demonstrated fairly good flow properties (Table 6). Flow properties became slightly worse as the ds value of starch acetates increased. This might be due to the more irregular particle shape and a larger fraction of smaller particles. Flowability and the angle of repose for of starch acetates were within the same range as MS, which is used as a direct compression filler. DCP had slightly better flow properties than the starch acetates. Based on the angle of repose (≤ 25°C), all studied starch acetate powders were freely flowing (Table 4 and 6). These results indicated that the flow properties of starch acetates are suitable for direct compression.

In general, starch acetate is an amorphous material, of which hydrophobicity increases with the acetyl content on the polymer backbone. It was found that drying methods had a relevant effect on the particle and powder properties of starch acetate. This gives an opportunity to modify particle and powder properties of starch acetate for different purposes.

5.4 Tableting of starch acetate (I, II, III)

5.4.1 Relative densities of powders (II)

It has been shown that both the particle size and shape have a great impact on relative density values (York 1978, Munoz-Ruiz and Paronen 1996). Relative densities (D_0, D_b, and D_A) of powder beds at the beginning of the compression phase in the present study are shown in Table 7. The rank order of different powder D_0 values was equal for tap densities. The greatest D_0 values, or the most densified powder packing due to the die filling, were found for batch 2, as predicted by the particle and powder properties (Table 6). D_0 values for batches 1 and 3 were the lowest. Variations in values were due to particle size; i.e., resulting in large void spaces between spherical particles, like those found with batch 1 and unfavorable particle and powder properties in batch 3.

The high D_b values of batches 1 and 3 were caused by fragmentation of the larger particles in batch 1 powder and disintegration of granules or agglomerates in batch 3 during the rearrangement phase. Batch 2 did not seem to exhibit particle rearrangement (D_b) at all. The most probable explanation for this unlikely observation is that particle

rearrangement already took place under a force of 100 N and, thus, this part of D_b was actually higher, and D_0 was lower. D_A values of all batches were practically equal.

Values of D_b and D_A for all starch acetate batches were considerably smaller than those of reference powders. Low D_b values are typically indicative of plastically deforming materials (Doelker 1988, Nyström et al. 1993). Although the particle and powder properties of MCC were predicted to be poor by means of die filling and rearrangement, the small applied force, which took place in D_0 measurement and unexpected excessive particle rearrangement, lead to well-densified powder packing at the beginning of compression.

Table 7. Compression and Tablet Properties*

Drying Method	D_0	D_b	D_A	P_Y (MPa)	Elastic Recovery (%)	Porosity (%)	Tensile Strength (MPa)
Batch 1	0.29	0.11	0.39	57	24.5	18.5	9.7
	(<0.01)	(0.01)	(0.01)	(2)	(0.7)	(0.3)	(0.5)
Batch 2	0.41	0.00	0.41	64	25.1	20.3	9.5
	(<0.01)	(0.01)	(0.01)	(1)	(1.2)	(0.6)	(0.4)
Batch 3	0.29	0.13	0.42	66	20.8	17.4	17.5
	(<0.01)	(0.01)	(0.01)	(1)	(1.0)	(0.6)	(0.5)
Batch 4	0.33	0.05	0.38	54	20.1	14.9	18.1
	(<0.01)	(0.01)	(0.01)	(<1)	(0.6)	(0.5)	(0.4)
MCC	0.30	0.30	0.61	129	11.1	18.2	15.6
	(<0.01)	(0.01)	(0.01)	(3)	(0.2)	(0.2)	(0.5)
DCP	0.44	0.28	0.72	267	5.1	18.0	3.6
	(<0.01)	(<0.01)	(<0.01)	(7)	(0.5)	(0.2)	(<0.1)

*SDs presented in parentheses.

5.4.2 Tablet compression (II)

The effects of particle properties and water content of the starting material on the volume reduction behavior during compaction, and the strength of compacted tablets have been extensively described by several authors (e.g., Ahlneck and Alderborn 1989, Karehill et al. 1990, Wong and Pilpel 1990, Malamataris and Karidas 1994, Nokhodchi et al. 1995). In general, a decrease in particle size, an increase in particle surface roughness and an optimal presence of water in the powder mass will result in stronger tablets, especially with plastically deforming materials. These properties facilitate the volume reduction of powder mass during compaction, resulting in a closer packing of particles in the compact, which leads to a greater bonding surface area to form bonds between particles and, subsequently, to higher compact strength.

Mean yield pressure (P_y) values of starch acetates varied between 54 and 66 MPa (Table 7). Values were approximately half that of MCC, which is known to deform easily by plastic flow. Thus, all starch acetate powders deformed easily under compression, and this result was consistent with the D_b results.

5.4.3 Tablet strength (I, II)

Starch acetates **(I)** having a low ds (0.34) already formed clearly stronger tablets than the reference tablet excipients. When ds was increased above 0.34; i.e., 1.19, tensile strength of the starch acetate tablets proved to be overwhelming when compared to other tested excipients, excluding MCC, which is generally known to have excellent binding properties (Fig. 16) (Doelker 1993).

When comparing different starch acetates **(I)**, it was found that high ds values resulted in stronger tablets that were essentially formed. Starch acetate ds 2.9 formed the strongest tablets under all studied compression pressures. Starch acetates with ds 1.19 and 2.1 formed almost equally strong tablets as ds 2.9, whereas ds 0.34 tablets were the weakest of all. The SEM micrographs of tablet surfaces showed the surface structure of different excipient tablets after compression (Fig. 15). On the surfaces of MCC, MS and low ds (0.34 and 1.19) starch acetate tablets, the interparticulate borderlines were still visible after compression. With higher ds (2.1 and 2.9) starch acetate tablets, neither interparticulate borderlines nor separated deformed particles could clearly be seen. Possible explanation is that the starch acetate of high ds simple makes well-compressed tablets with only small pores. Tablets made of starch acetate ds 2.1 and 2.9 were monolithic, homogenous and formed a very firm polymer matrix, with a smooth surface and without any clearly visible particule borderlines (Fig. 15).

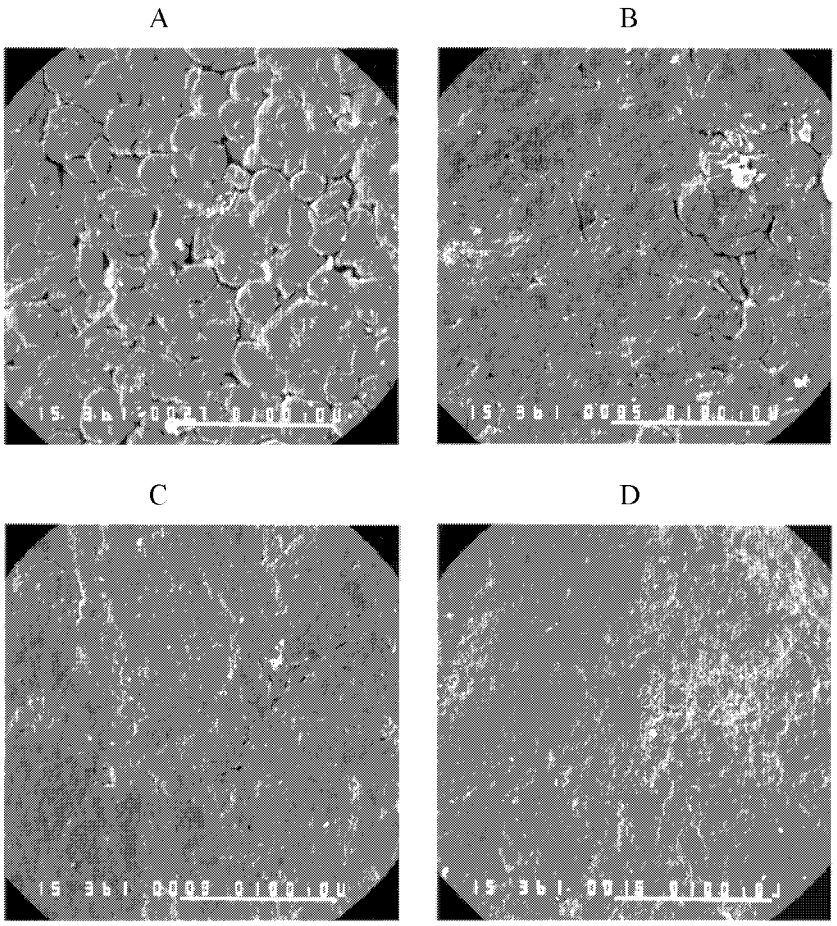

Figure 15. The SEM micrographs of starch acetate tablet surfaces with ds 0.34(A), ds 1.19(B), ds 2.1(C), and ds 2.9(D). Compression force was 25 kN. The reference bar is 100 μm.

The effects of particle and powder properties on the strength of starch acetate tablets can be seen in differently dried starch acetates **(II)** (Table 5, 6 and 7). Tablets made from batches 3 and 4 were the strongest, having a small particle size, irregular particle shape, greater particle surface roughness, the largest specific surface area and moderate to high water content. It can be assumed that in batches 3 and 4 there were numerous contact points and a large bonding surface area to form strong interparticular bonds between the particles, and subsequently firmer tablets. Tablets made from batches 1 and 2 formed considerably weaker tablets. Particle and powder properties of these powders

were unfavourable for interparticular bond formation during compaction. This situation leads to high porosity and elastic recovery, and consequently weaker tablets.

5.4.4 Characteristics of tablet (I, II)

Although the final porosity of the tablets **(II)** was almost equal between starch acetates and MCC, tablets made from starch acetate powders expanded by approximately two fold more after compression, compared to tablets made from MCC (Table 7). However, interparticulate bonds formed in starch acetate tablets were strong enough to allow the stress relaxation without breakage of the tablet (e.g., capping) and still, tablets made from batches 3 and 4 were stronger than tablets compressed from MCC. This observation indicated an overwhelming interparticular bond formation capacity for starch acetate.

Friability **(I)** results were in agreement with mechanical strength results of tablets made from starch acetates. Ds 2.9 tablets had the smallest weight loss at all studied compression pressures. All starch acetate and MCC tablets met the limits of the Ph.Eur. test for loss of weight.

In tablet disintegration tests **(I),** all tablets made of starch acetate ds 0.34 were completely disintegrated within a few minutes, while tablets made of starch acetates ds 2.1 and 2.9 at compaction pressure of 190 MPa or higher did not disintegrate at all during the measurement time of two hours (Fig. 16).

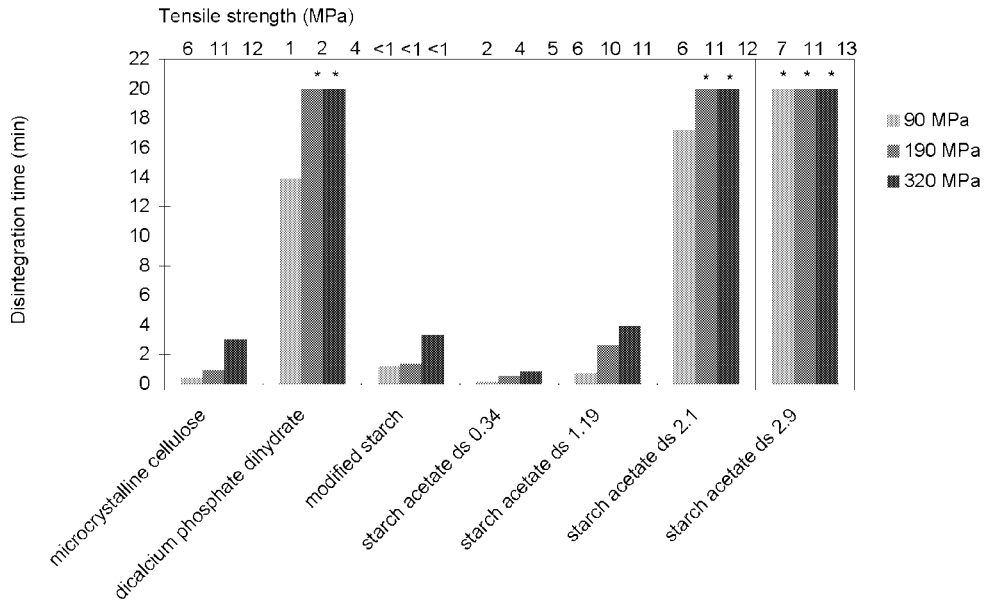

Figure 16. Disintegration times and tensile strengths of tablets. (* = did not disintegrate within 2 hours)

Tableting studies demonstrated that starch acetates are easily deforming excipients under pressure. Deformation properties consist of both plastic and elastic deformations. In spite of elasticity, starch acetate have excellent binding capacity to form firm tablets. In particular, starch acetate having a high degree of substitution exhibit overwhelming mechanical strength properties.

5.5 *In vitro* drug release from starch acetate tablets (I, III, IV)

In the preliminary dissolution studies, propranolol was used as a model drug. The dissolution rate **(I)** of propranolol changed from rapid release (i.e., low ds) to sustained release (i.e., high ds) (Fig. 17). Propranolol was released from starch acetate tablets with ds values of 0.34 and 1.19 within a few minutes. The rapid drug release rates can be attributed to the short disintegration time of the tablets and, thus, immediate dissolution of propranolol. Starch acetate ds 2.1 and 2.9 tablets demonstrated extended release profiles with a small initial burst effect, where drug particles from the tablet surface dissolved rapidly after contact with the dissolution medium. The tested reference excipients did not have any release controlling properties, as expected. These results indicate that the drug release mechanism from high ds, intact and monolithic tablets was

diffusion, where water penetrates at a slow rate into the tablet pores, causing Fickian diffusion of propranolol through the formed water channels.

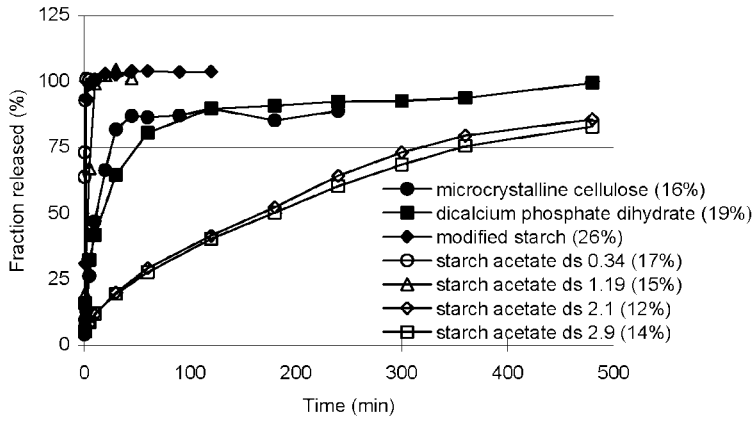

Figure 17. Propranolol-HCl release from various tablets

Drug release **(III)** from high ds starch acetate (ds 2.7), with physicochemically different drugs, was also studied. Nine different dissolution profiles for each model drug were generated by using a similar dissolution method in all cases (Table 2).

After obtaining profiles (Fig. 18), the fraction release (%) was fitted by the Power Law equation for up to 60 % of the fraction released. The drug release diffusional exponent (n) varied between 0.39 – 0.95, and more typically between 0.44 – 0.80. The goodness of fit (r^2) was at least 0.98 in each case, and in most cases it was ≥0.99. As the release kinetics of formulations deviated (0.39-0.95) considerably from Fickian diffusion (n=0.45), drug release rates (k) could not be compared excluding at the time point 1 hour. Results agreed with Pohja et al. (2003); i.e., different kinds of drug release kinetics exist when starch acetate was used as a release-controlling excipient. Thus, dissolution profiles were roughly divided to four classes (A to D), according to the diffusional exponent n; profiles in class A (n<0.45), B (0.45≤n≤0.50), C (0.50<n≤0.60), and D (n>0.60).

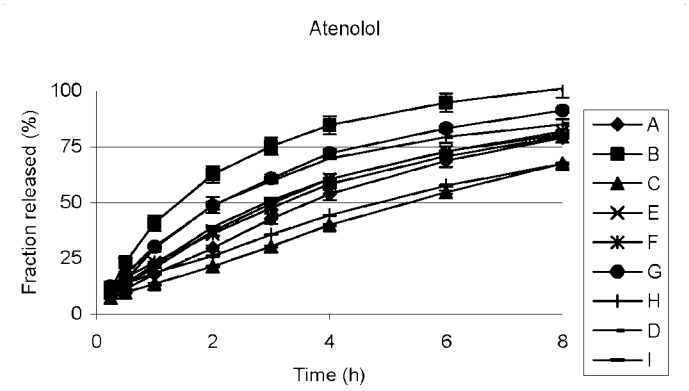
Atenolol
Fraction released (%)
100
75
50
25
0
0
2
4
6
8
Time (h)
A
B
C
E
F
G
H
D
I

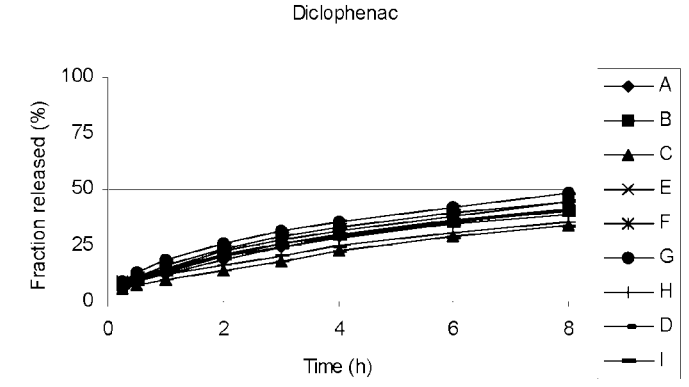
Diclophenac
Fraction released (%)
100
75
50
25
0
0
2
4
6
8
Time (h)
A
B
C
E
F
G
H
D
I

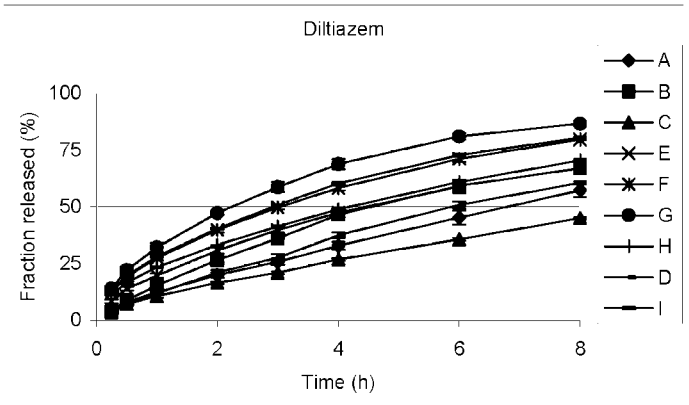
Diltiazem
Fraction released (%)
100
75
50
25
0
0
2
4
6
8
Time (h)
A
B
C
E
F
G
H
D
I

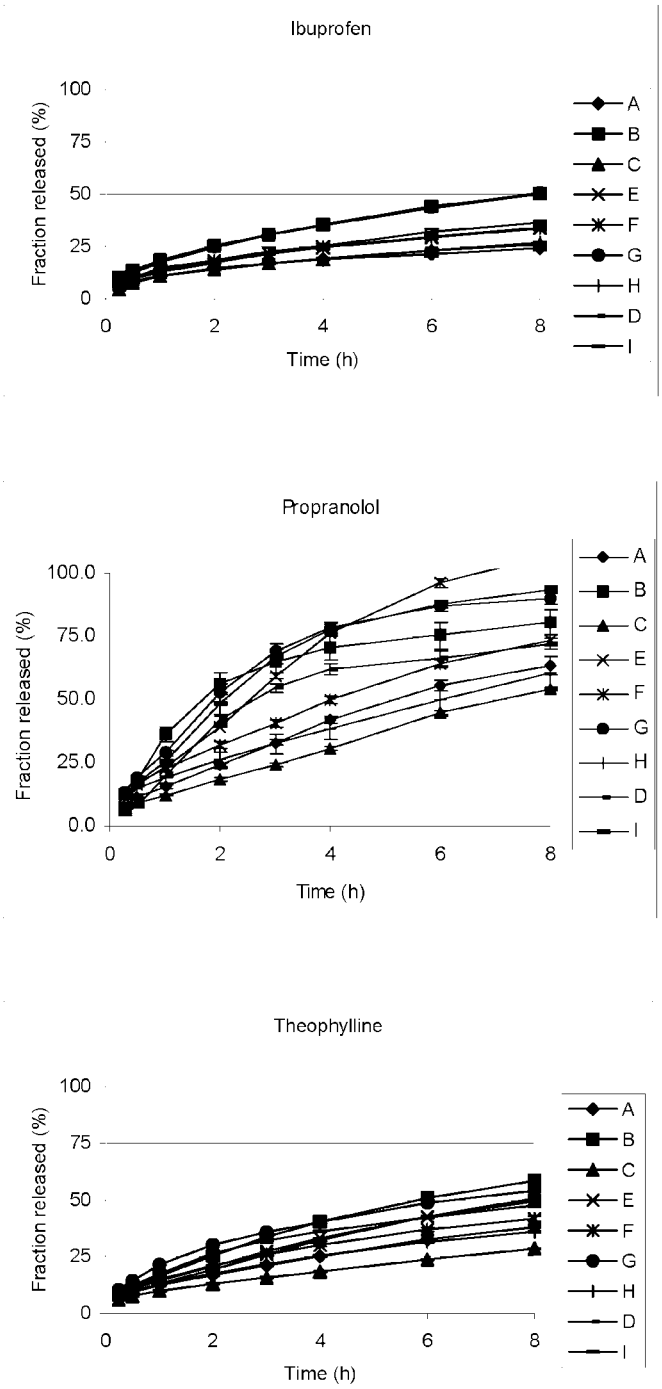

Figure 18. Dissolution profiles of different model drugs.

Pohja et al., (2003) found that under certain circumstances, starch acetate tablets laminated or cracked during dissolution tests, which increased porosity and the available surface area for dissolution, decreased tortuosity, and consequently, caused the deviation from Fickian diffusion release (Fig. 19). Same kind of phenomenon has been observed with amylodextrin (Steendam et al. 2000). To clarify this, dissolution profiles were plotted in different scales (i.e., normal time and the square root of time). This method was found to be very useful in characterizing dissolution profiles, which deviated from Fickian diffusion. This resulted in the first observation that a burst effect existed for each formulation at the beginning of dissolution (0-1 hour) (Fig. 20A). This was understandable, as compacts were matrix tablets compressed from a binary mixture of drug and starch acetate. Thus, drug particles from the surface of a tablet were able to dissolve without any control by starch acetate.

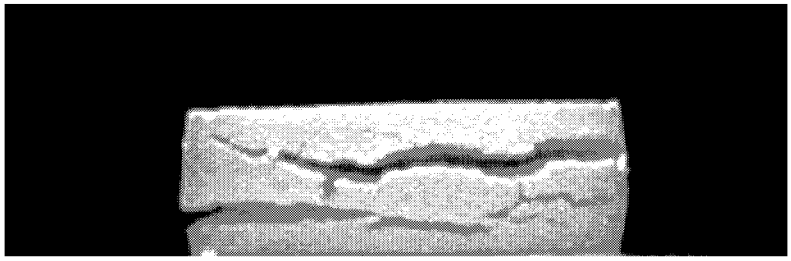

Figure 19. Cracked tablet after dissolution test.

Interestingly, profiles in classes A, C and D were nearly equal during the burst effect, up to 1 hour, but then they deviated considerably from each other (Fig. 20B). The release kinetics remained as diffusion in classes A and C, but the diffusion rate constants changed and, surprisingly, profiles in class D followed constant drug release. This means that drug release from starch acetate tablets gradually changes after the burst effect from diffusion, with increasing rate constants, towards constant drug release. These gradual changes were assumed to strongly related to crack formation. To calculate drug release rates, the burst effect (0-1h) was excluded before fitting. Release profiles in classes A, B and C were plotted against the square root of time, and slopes were used as diffusional release rate constants (Kh, $h^{-0.5}$). Release profiles in class D were plotted against normal time scales, and the slopes were used as zero-order release rate constants (Kz, h^{-1}).

A

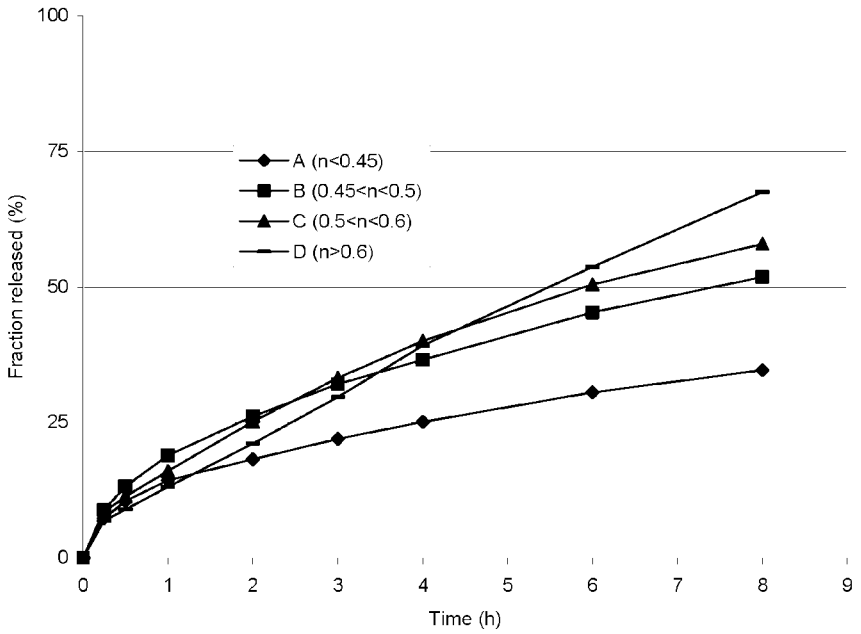

B

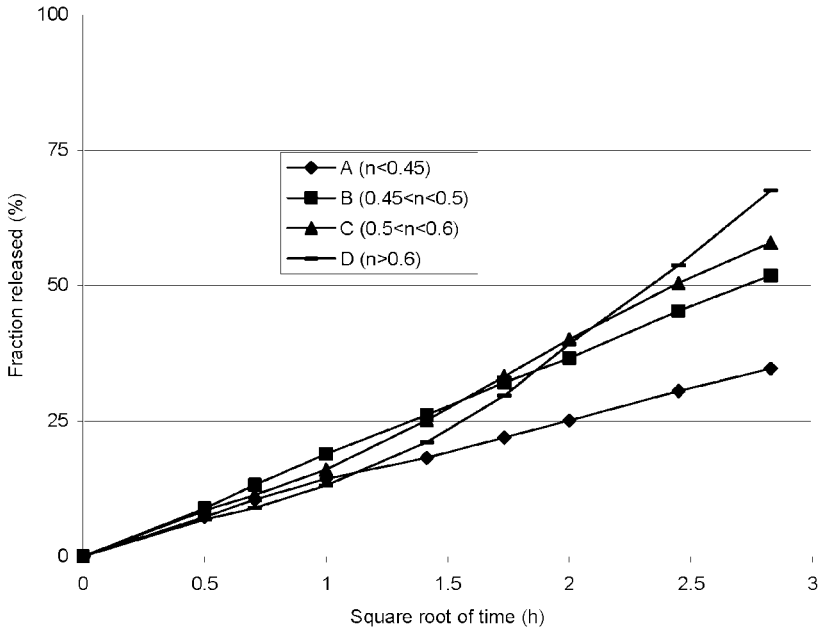

Figure 20. Release profiles against normal time scale (A), and the square root of time (B).

5.6 Multivariate data analysis in the evaluation of drug release from tablets (III)

5.6.1 Principal Component Analysis (PCA) (III)

PCA was used to describe the entire data set. The description of a total data matrix was accomplished with eight PCs to model the variance (r^2 = 0.93, Q^2 = 0.84). The resulting PCA score plot indicates that some strong outliers and a few possible outliers were found. Outliers having extreme values of n (n<0.45 and n>0.82) were excluded from further analysis. According to the PCA loading plot, drug properties were more related to a second main component, whereas the first component described the tableting and tablet properties. PCA also provided a strong positive correlation between n value and several drug properties, and a negative correlation between the n value and tablet properties.

5.6.2 Partial least squares to latent structures (PLS) (III)

PLS was first applied to the drug release diffusional exponent (n). After removing outliers and insignificant variables, the number of observations (n) and significant variables was 125 and 24, respectively. The constructed model (using four PCs) was able to fit (r^2=0.83) and predict (Q^2=0.78) variance of the diffusional exponent. Also, there was a good linear relationship between the observed and predicted values of n (r^2=0.83) (Fig. 21A). Next, release rate constants Kh and Kz were analysed. Profiles belonging to classes B and C were analysed together, as they were assumed to follow the same release mechanism. To analyse diffusional rate constants (Kh), two PCs with six significant variables and 87 observations were used (r^2=0.79, Q^2=0.75). The correlation between the observed and predicted rate constants was r^2=0.79 (Fig. 21B). In the case of zero-order release rate constants (Kz), the first PC was able to construct the model (r^2=0.84, Q^2=0.84) already with five variables. Furthermore, a correlation between observed and predicted rate constants was calculated to be r^2=0.79 (Fig. 21C).

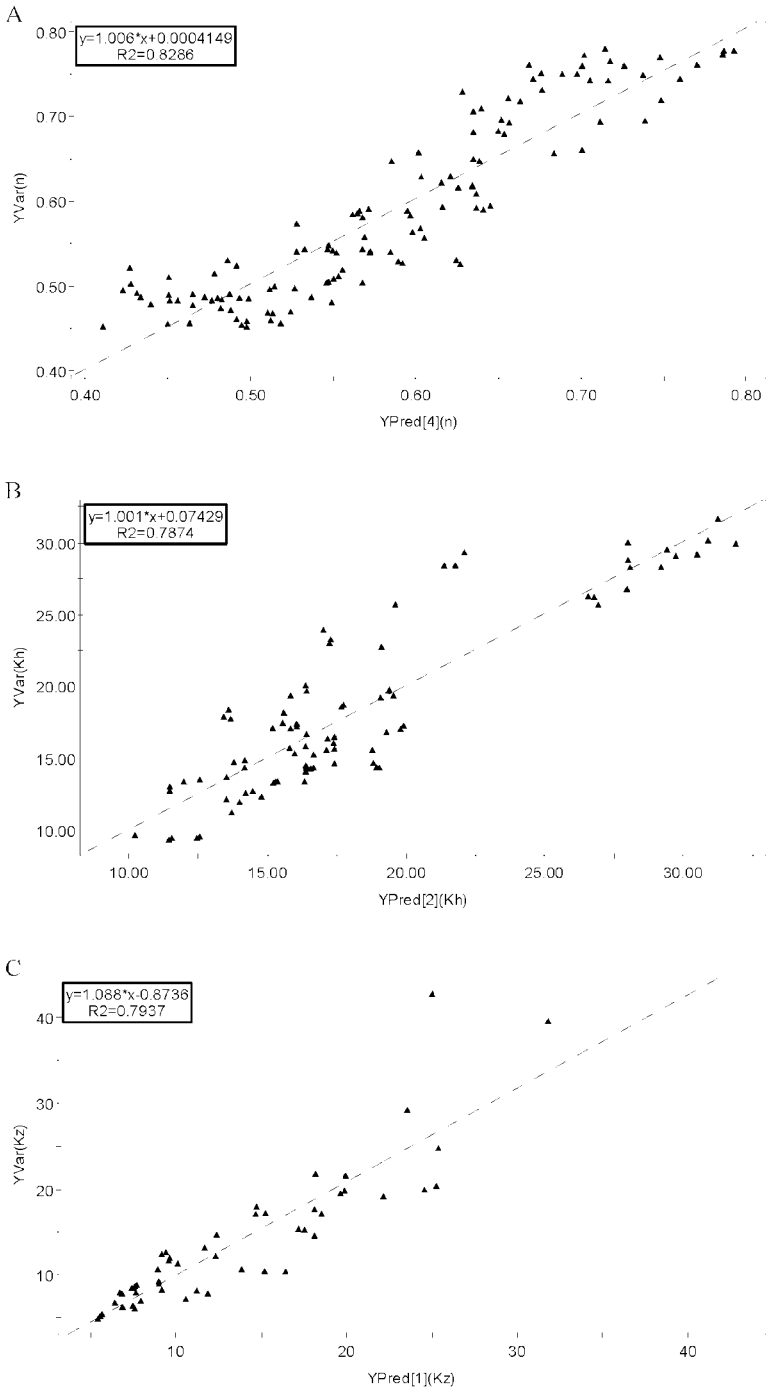

Figure 21. Predicted versus observed values for the diffusional exponent n (A), diffusional drug release rates ($0.45<n<0.6$) (B) and constant drug release rates ($n>0.6$) (C) using PLS modeling.

5.6.2.1 Drug release kinetics (III)

As PCA previously indicated, the most descriptive variables for explaining the variation of diffusional exponent were related to drug properties (Fig. 22). Increasing molecule flexibility (Flex) and hydrogen bonding capacity (HB, HBAo and HBD) tended to change the drug release mechanism towards anomalous or even zero-order drug release. Drug lipophilicity (Log P, Log D(6.8)) and molecule weight (FW) had an opposite effect; i.e., as they decreased, the value of *n* increased. The most descriptive tablet variable was elastic recovery (ER%). Thus, the impact of variables came from two origins; one from the drug chemistry, and second from the structural property of the tablet. Variables that controlled diffusional release were mostly of chemical origin, while tablet or tableting properties controlled drug release in constant drug release. However, these results cannot be explained without taking into account the analysis of rate constants. Thus, the effect of variables on release kinetics and rate constants must be analysed simultaneously.

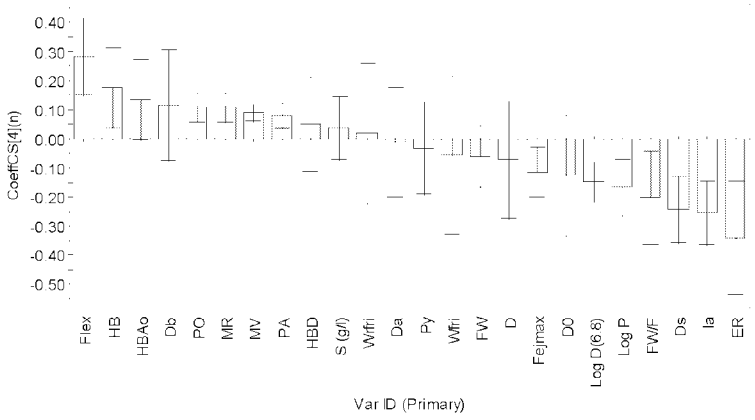

Figure 22. PLS coefficient plot for the correlation of variables with diffusional exponent *n*.

5.6.2.2 Diffusional drug release rates (III)

By using certain formulae and tableting conditions, starch acetate forms structurally inert hydrophobic matrix tablets, and drug release follows Fickian diffusion ($0.45<n\sim0.60$). Drug molecules with a high degree of flexibility, large amounts of hydrogen bonding acceptors and a small molecular volume tend to release a drug faster

than rigid, big and hydrogen-donor rich molecules (Fig 23). The positive effect of HBAo on drug release rate is assumed to be due to the electrostatic repulsion between the hydrogen bond acceptor of a drug molecule and starch acetate, a starch acetate consists almost entirely of hydrogen acceptors. Thus, it is assumed that the drug molecule, which typically contains several hydrogen bond acceptor sites, preferably diffuses out from the starch acetate matrix through water channels, rather than residing in the hydrogen acceptor-rich wall of the channel. The weight and elastic recovery of tablets were the most significant tablet variables. These parameters are related to the geometry of a tablet, and thus diffusional drug release rates.

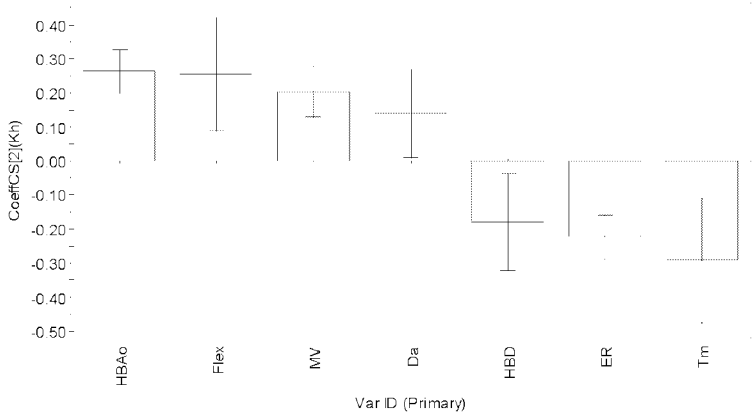

Figure 23. PLS coefficient plot for the correlation of variables with diffusional drug release rates ($0.45<n<0.6$).

5.6.2.3 Constant drug release rates (III)

In Fickian diffusion, the structural properties of tablets play only a minor role, but as drug release kinetics proceed towards constant drug release, structural properties became dominant. Results from the analysis of zero-order rate constants ($n>0.6$) indicated that release rates could be described by tableting and tablet variables, without any drug variables. Thus, the structural changes of the tablet governed drug release rates as $n>0.6$.

The following variables controlled zero-order rates in the present study, and were related to the formation of the release controlling matrix; elastic recovery of tablets (ER%), upper punch work (W_{up}), net work of compaction (W_{net}), yield pressure (P_y) and tablet porosity (Tp) (Fig. 24). W_{up} describes the total energy that is applied to the tablet by the upper punch during compaction. W_{net} of compaction describes the energy that is

consumed by the formation of interparticular bonds during compaction. In the present study, the value for drug release rate constants increased as the net work and/or upper punch work decreased and tablet porosity (Tp) increased. In other words, decreased energy input for interparticular bond formation leads to imperfect matrix formation and subsequent increased drug release rates.

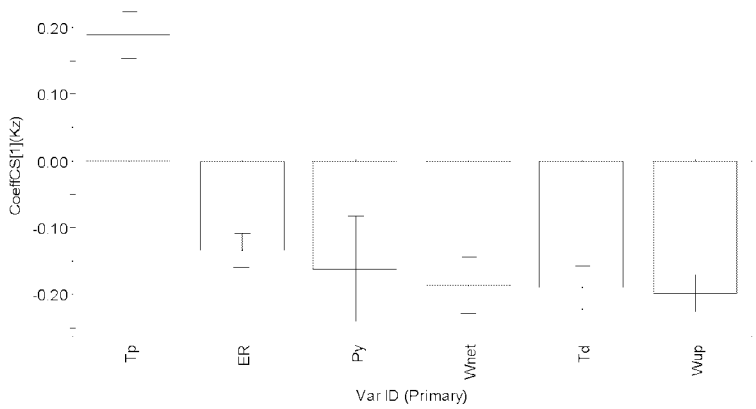

Figure 24. PLS coefficient plot for the correlation of variables with constant drug release rates (n>0.6).

A surprising observation was the effect of tablet elastic recovery (ER) on drug release kinetics and rate constants. To understand the effect of elasticity on drug release in the case of starch acetate, a larger scope was adopted. Raatikainen et al., (2002) and results in Table 6 indicate that starch acetate is a rather elastic material (Young's modulus approximately 3 GPa), having both a low yield pressure (50-70 MPa) and large elastic recovery (20-25%). Yield pressure describes the deformation properties of the material. Low yield pressure values indicate an easy densification of a material under pressure. It should be noted that the yield pressure value consists of a plastic deformation component and an elastic component. This elasticity can recover fast in the die or slowly during storage. In the present study, elastic recovery (ER%) was described in both cases. Keeping this in mind, the lamination or crack formation during dissolution, and the effect of elasticity on drug release, can all be explained and understood.

Thus, under certain circumstances, it is possible to formulate drug – starch acetate tablets that follow constant drug release kinetics. In such cases, a suitable amount of elastic energy (low P_y) must be loaded into the tablet during tableting, but tablets are

strong enough to resist elastic recovery. When tablets are immersed in a dissolution medium, water starts to penetrate through the pores into the tablets. Water breaks down interparticular bonds and tablets begin expanding, due to the recovery of loaded elastic energy, which causes lamination or crack formation (Fig. 19). Crack formation dramatically increases the surface area available for the dissolution of a drug, and decreases the diffusion path length and tortousity (Pohja et al., 2003). When crack formation and the increase of surface area is synchronized with time, constant drug release can be achieved. It should be mentioned that the total elasticity of a tablet is a combination of starch acetate elasticity and the drug. Thus, if the elasticity of starch acetate and a drug is different enough, microscopic crack formations can occur already in the dry state, which facilitates cracking during dissolution.

5.7 Bioavailability (IV)

In the present study, starch acetate-based direct compression tablets were administered to humans for the first time in a pharmacokinetic study (n=9). Three different starch acetate – diltiazem formulations had clearly different diltiazem plasma profiles (Fig. 25, Table 8). The same rank order existed between *in vitro* and *in vivo* profiles, and C_{max} and $AUC_{0-\infty}$ decreased as the *in vitro* dissolution drug release rate decreased, which confirms that starch acetate is able to control drug release from tablets in humans.

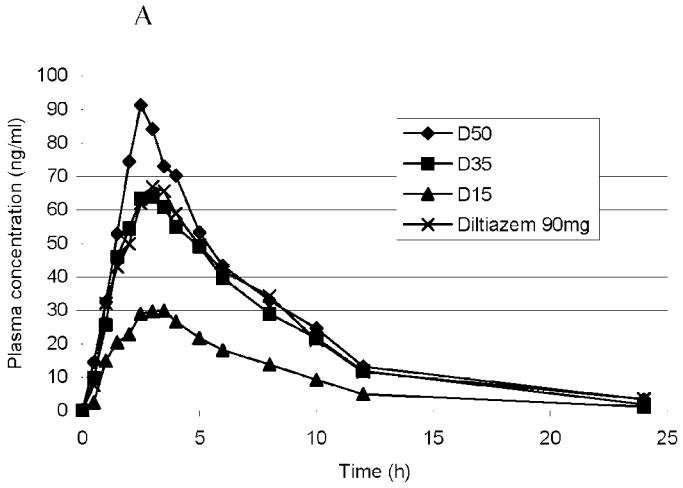

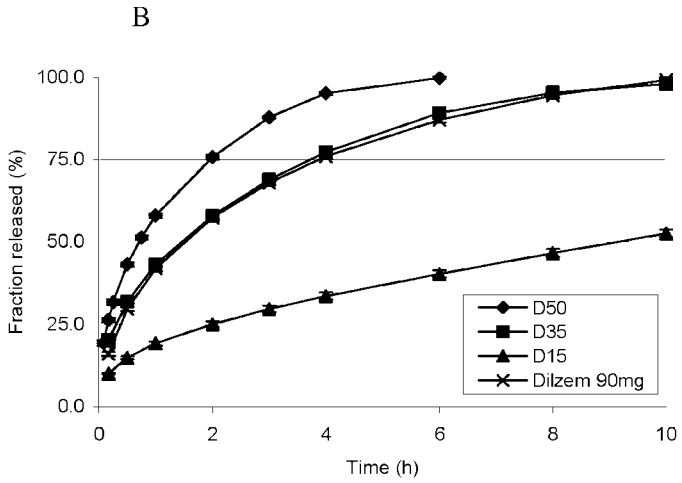

Figure 25. *In vivo* drug plasma concentrations (A) and *in vitro* drug release profiles (B). Formulations consist of diltiazem (90 mg) 50% (D50), 35% (D35) and 15% (D15).

Table 8. Pharmacokinetic parameters (n=9)*.

	C_{max} (ng/ml)	$AUC_{0-\infty}$ (ng·h/ml)	T_{max}[a] (h)	MRT[b] (h)
D 50	95.4 (14.4)	609.5 (174.4)	2.6 (0.6)	6.2 (1.5)
D 35	68.8 (23.5)	510.7 (189.8)	2.8 (0.5)	6.5 (1.2)
D 15	31.1 (8.0)	231.4 (107.4)	3.0 (0.5)	5.9 (1.5)
Dilzem 90 mg depottabl	70.7 (18.0)	532.6 (195.0)	3.5 (0.5)	6.5 (1.5)

[a] time of the C_{max}
[b] mean residence time
*SDs presented in parentheses.

5.7.1 *In vitro – In vivo* correlation (IVIVC) (IV)

Diltiazem follows at least a two-compartment model after intravenous administration (Hoglund and Nilsson 1989). Therefore, the Wagner-Nelson method cannot be used for the establishment of IVIVC. Deconvolution methods and the Loo-Riegelman method are commonly used to analyse IVIVC for 2-compartment model drugs (Qiu et al. 2000). Since the reference administration (e.g., intravenous or an oral solution) is needed in these methods, an alternative method was used to establish IVIVC, without any reference administration.

Establishment of IVIVC was initiated by plotting the mean *AUCcum(t)* against time and fitting those curves to the Hill equation. Generated Hill equations fit well with the *AUCcum(t)* profiles ($r^2 > 0.99$), and each constant was statistically significant (Fig. 26). Constants *b* and *c* were almost similar and independent of formulation, while constant *a* was strongly dependent on formulation (Table 9). After that, the mean values of constants *b* and *c* were used, and constant *a* was used to describe *AUCcum(t)* profiles (Eq. 20).

$$AUCcum(t) = \frac{a \cdot t^{1.99}}{5.55^{1.99} + t^{1.99}} \qquad (20)$$

According to the correlation analysis, there was a strong positive correlation between *in vitro* drug release rate (*k*) and *in vivo AUCcum(t)*, described by Hill's constant *a*, and the following linear regression equation was obtained between them (Eq. 21):

$$a = 10.4 \cdot k + 45.6 \qquad (r^2 = 0.993) \qquad (21)$$

Table 9. *In vitro* release parameters of Power Law equation and fitted Hill parameters for *AUCcum(t)*, and prediction error (%PE) values for $AUC_{0\text{-}24}$ and C_{max}.

	In vitro constants		In vivo Hill's constants			Prediction error %	Prediction error %
	Rate constant (k)	Diffusional exponent (n)	a	b	c	C_{max} (ng/ml)	$AUC_{0\text{-}24h}$ (ng·h/ml)
D50	57.27	0.42	620.1	1.94	5.43	-19.3	-1.7
D35	43.15	0.42	512.7	2.01	5.61	-9.7	-8.2
D15	18.98	0.43	197.4	2.02	5.62	-5.4	-0.4
Mean	-	0.43	-	1.99	5.55	-11.4	-3.4
Standard deviation	-	0.01	-	0.04	0.11	7.1	4.2

Evaluation of the internal predictability of IVIVC was based on calculations from the initial data sets (D15, D35 and D50). First, new Hill's constants *a* were determined using equation 21 and *in vitro* drug release rate constants (*k*) for each formulations. Next, predicted *AUCcum(t)* profiles were generated using equation 20 and respective new Hill's constants *a* (Fig 26). Finally, predicted plasma concentrations were rehabilitated from the predicted *AUCcum(t)* values (Fig 27). Prediction errors on $AUC_{0\text{-}}$

$_{24h}$ and C_{max} for each formulation are presented in Table 9. All formulations reached the acceptance limits except the C_{max} of D50, which was outside of the 10% acceptance limit.

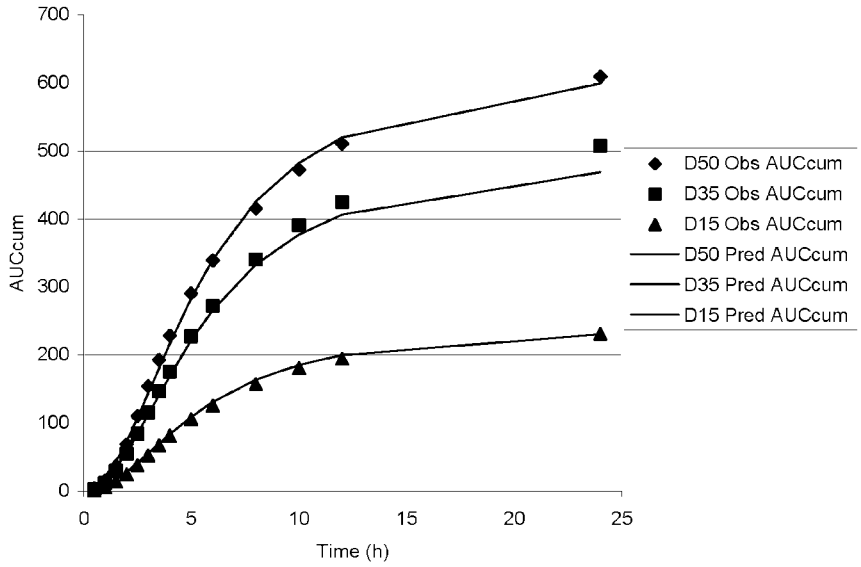

Figure 26. Cumulative AUC of different formulations and the predicted AUCcum of different formulations (solid lines). Formulations consist of diltiazem (90 mg) 50% (D50), 35% (D35) and 15% (D15).

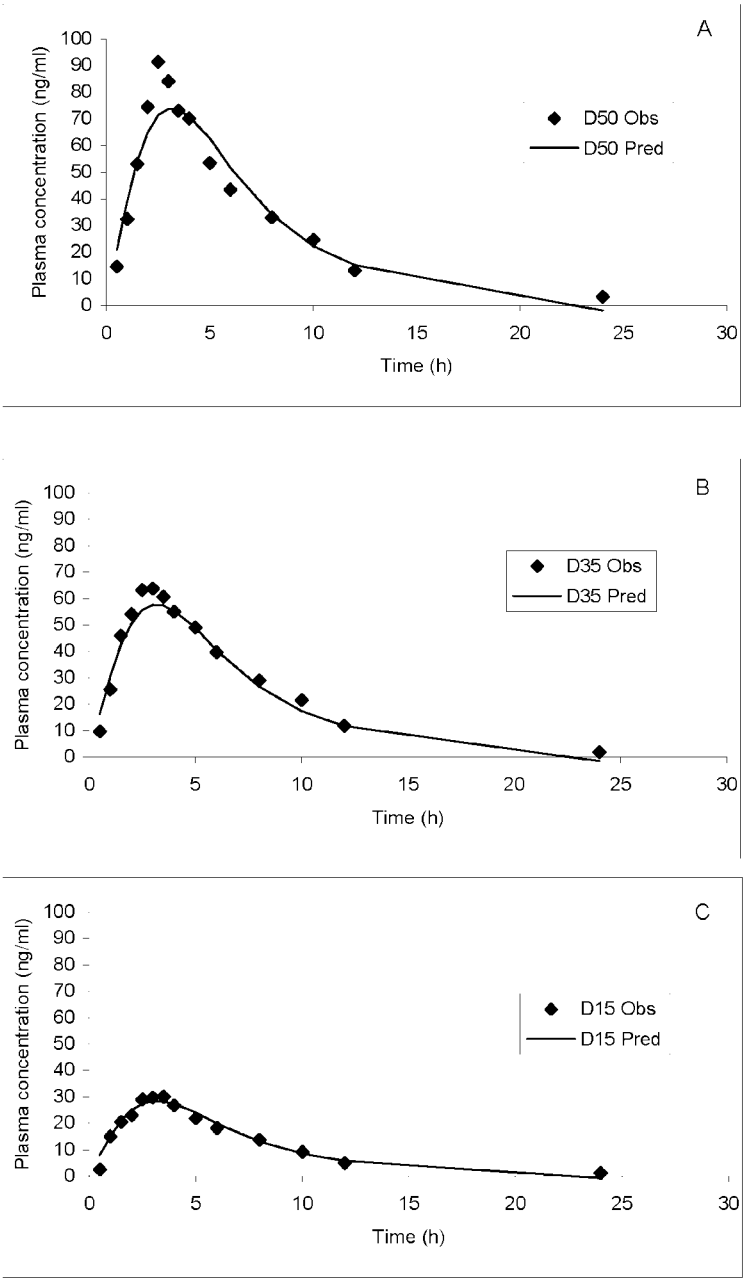

Figure 27. Diamonds are observed plasma concentrations and solid lines are predicted plasma concentrations. Formulations consist of diltiazem (90 mg) 50% (D50), 35% (D35) and 15% (D15).

IVIVC was established without any reference administration of diltiazem, which follows multicompartmental pharmacokinetics, extensive first pass metabolism and large inter-subject variability. The combination of the cumulative AUC, the Hill equation and correlation and regression analyses enabled the establishment of a predictive IVIVC. Advantages of established IVIVC are direct determination of final plasma concentration (and cumulative AUC) of drug instead of indirect estimation of drug absorption, and simple mathematics. However, the predictive AUC_{0-24} and C_{max} values were slightly underestimated, and thus, it might be beneficial to test alternative mathematical equations for the descriptions of profiles. In present study, it should be noted that *in vitro* drug release profiles followed same release mechanism, which simplified the generation of IVIVC. If the release mechanism changes between formulations, it might affect more complicated relationships between *in vitro* and *in vivo* profiles, and difficulties to find reasonable parameters to describe *in vitro* and *in vivo* profiles.

5.7.2 Bioequivalency (IV)

In vitro and *in vivo* profiles demostrated that D35 was nearly superimposable with the reference profiles, which gave an impression that bioequivalence might have been achieved (Fig. 26). However, bioequivalency data showed that the 90% confidence intervals for $AUC_{0-\infty}$ and C_{max} values slightly exceeded the acceptable limits for bioequivalency (0.80-1.25).

6 CONCLUSIONS

The present study introduced a novel excipient (starch acetate) for extended oral drug release. It can be concluded that starch acetate is applicable for this purpose. It possesses suitable particle and powder properties for direct compression tableting, and it is capable of extending drug release in a simple way. In addition, multivariate data analysis was shown to be valuable tool for evaluating of drug release from tablets. Furthermore, a predictive IVIVC model could be establish by using an alternative approach. The specific conclusions can be listed as follows:

1. Most physicochemical properties of starch acetates are related to the degree of acetyl substitution. As the degree of the acetyl moiety increase, starch acetate becomes more hydrophobic, mechanical strength increases and disintegration does not occur anymore. As a result drug release form these tablets goes towards extended release.

2. The particle and powder properties can be affected by different drying processes. Critical points are mixing and the method of water removal. Fluidization techniques produce small, irregular and rough particles having moderate powder characteristics, but excellent tablet properties, whereas vacuum techniques produce larger, spherical and smooth particles with excellent powder characteristics but only moderate tablet properties. In tabletting, starch acetate shows typical visco-elastic compaction behaviour.

3. Drug release from tablets prepared from drug-starch acetate binary mixtures varies from the Fickian diffusion to anomalous or even zero-order transport of drug according to Power Law equation. Important factors that were relevant to managing diffusional drug release from starch acetate tablets, were based on the chemistry of the drug, especially molecule flexibility, hydrogen bonding capacity, partition coefficient and molecule size. Important tablet descriptors that described the matrix structure were especially elasticity and consequent lamination or cracking of tablets, which were governed by zero-order drug release.

4. Different release profiles created *in vitro* were also found in humans, which confirm that starch acetate is able to control and extend drug release *in vivo*. IVIVC was established without any reference administration of diltiazem, which follows multicompartmental pharmacokinetics, extensive first pass metabolism and large inter-subject variability. The combination of the *in vivo* cumulative AUC and *in vitro* drug release profiles described by the Hill and Power Law equation, respectively, enabled the establishment of a predictive IVIVC.

7 REFERENCES

Adams E, De Maesschalck R, De Spiegeleer B, Vander Heyden Y, Smeyers-Verbeke J, Massart DL: Evaluation of dissolution profiles using principal component analysis. Int J Pharm 212: 41-53, 2001

Adams E, Walczak B, Vervaet C, Risha PG, Massart DL: Principal component analysis of dissolution data with missing elements. Int J Pharm 234: 169-178, 2002

Ahlneck C, Alderborn G: Moisture adsorption and tabletting. I. Effect on volume reduction properties and tablet strength for some crystalline materials. Int J Pharm 54: 131-141, 1989

Amidon GL, Lennernäs H, Shah VP, Crison JR: A theoretical basis for a biopharmaceutic drug classification: the correlation of in vitro drug product dissolution and in vivo bioavailability. Pharm Res 12: 413-419, 1995

Atkinson RM, Bedford C, Child KJ, Tomich EG: Effect of particle size on blood griseofulvin levels in man. Nature 193: 588-589, 1962

Bakatselou V, Oppenheim RC, Dressman JB: Solubilization and wetting effects of bile salts on the dissolution of steroids. Pharm Res 8: 1461-1469, 1991

Balan G, Timmins P, Greene DS, Marathe PH: In vitro – In vivo correlation (IVIVC) models for metformin after administration of modified-release (MR) oral dosage forms to healthy human volunteers. J Pharm Sci 90: 1176-1185, 2001

Bataille B, Ligarski K, Jacob M, Thomas C, Duru C: Study of the influence of spheronization and drying conditions on the physico-chemical properties of neutral spheroids containing Avicel PH 109 and lactose. Drug Dev Ind Pharm 19: 653-671, 1993

Bates TR, Gibaldi M, Kanig JL: Solubilizing properties of bile salt solution I: Effect of temperature and bile salt concentration on solubilization of glutethimide, griseofulvin and hexestrol. J Pharm Sci 55: 191-199, 1966

Bergström CAS, Norinder U, Luthman K, Artursson P: Experimantal and computational screening models for prediction of aqueous drug solubility. Pharm Res 19: 182-188, 2002

Camenisch G, Folkers G, van de Weterbeemd H: Review of theoretical passive drug absorption models: Historical backround, recent developments and limitations. Pharm Acta Helv 71: 309-327, 1996

Cardot J-M, Beyssac E: In vitro-in vivo correlations: Scientific implications and standardization. Eur J Metab Pharmacokinet 1: 113-120, 1993

Chatrath M, Staniforth JM: The relative influence of dielectric and other drying techniques on the physico-mechanical properties of a pharmaceutical tablet excipient. Part I: Compaction characteristics. Drying Technol 8: 1089-1109, 1990

Colombo P, Bettini R, Massimo G, Catellani PL, Santi P, Peppas NA: Drug diffusion front movement is important in drug release control from swellable matrix tablets. J Pharm Sci 84: 991-997, 1995

Colombo P: Swelling –controlled release in hydrogel matrices for oral route. Adv Drug Deliv Rev 11: 37-57, 1993

Crank J: The mathematics of diffusion, 2nd ed. Clarendon Press, Oxford, England, 1975

Cutler DJ: Numerical deconvolution by least squares: Use of prescribed input function. J Pharmacokin. Biopharm 6: 227-241, 1978

De Blaey CJ, Polderman J: Compression of pharmaceutical: I. The quantitative interpretation of force displacement curves. Pharm Weekbl 105: 241-250, 1970

De Blaey CJ, Polderman J: Compression of pharmaceutical: II. Registration and determination of force-displacement curves, using a small digital computer. Pharm Weekbl 106: 57-65, 1971

Desai MP, Labhasetwar V, Amidon GL, Levy RJ: Gastrointestinal uptake of biodegradable microparticles: effect of particle size. Pharm Res 13: 1838-1845, 1996

Doelker E: Recent advances in tableting science. Boll Chim Farm 127: 37-49, 1988

Doelker E: Comparative compaction properties of various microcrystalline cellulose types and generic products. Drug Dev Ind Pharm 19(17&18): 2399-2471, 1993

Dressman JB, Berardi RR, Dermentzoglou LC, Russel TL, Schmaltz SP, Barnett JL, Jarvenpaa KM: Upper gastrointestinal pH in young, healthy men and women. Pharm Res 7: 756-761, 1990

Dressman JB, Amidon GL, Reppas R, Shah VP: Dissolution testing as a prognostic tool for oral drug absorption: Immediate release dosage form. Pharm Res 15: 11-22, 1998

Dyer AM, Khan KA, Aulton ME: Effect of the drying method on the mechanical and drug release properties of pellets prepared by extrusion-spheronization. Drug Dev Ind Pharm 20, 3045-3068, 1994

Dyrstad K, Veggeland J, Thomassen C: A multivariate method to predict the water vapour diffusion rate through polypropylene packaging. Int J Pharm 188: 105-109, 1999

Ebel JP: A method for quantifying particle absorption from the small intestine of the mouse. Pharm Res 7: 848-951, 1990

Efentakis M, Buckton G: The effect of erosion and swelling on the dissolution of theophylline from low and high viscosity sodium alginate matrices. Pharm Dev Technol 7: 69-77, 2002

Egan WJ, Lauri G: Prediction of intestinal permeability. Adv Drug Deliv Rev 54: 273-289, 2002

EMEA: Note for guidance on quality of modified release products: A: Oral dosage forms, B: Transdermal dosage forms, Section I (Quality), CPMP/QWP/604/96, July, 1999a

EMEA: Note for guidance on modified release oral and transdermal dosage forms: Section II (Pharmacokinetic and clinical evaluation), CPMP/EWP/280/96, July, 1999b

Eriksson L, Johansson E, Kettaneh-Wold N, Wold S: Multivariate- and megavariate data analysis: Principles and applications. Umetrics Academy, Umeå, Sweden, 2001

Evans DF, Pye G, Bramley R, Clark AG, Dyson TJ, Hardcastle JD: Measurement of gastrointestinal pH profile in normal ambulant human subjects. Gut 29: 1035-1041, 1988

FDA Guidance For Industry: Modified release solid oral dosage forms: Scale-up and Post Approval Changes (SUPAC-MR): Chemistry, Manufacturing and Controls; In Vitro dissolution testing and In Vivo bioequivalence documentation. September, 1997a

FDA Guidance For Industry: Extended release oral dosage forms: Development, Evaluation, and Application of In Vitro/In Vivo correlations. September, 1997b

FDA Guidance For Industry: Statistical approaches to establishing bioequivalence. 2001

Fell JT, Newton JM: Determination of tablet strength by the diametral-compression test. J Pharm Sci 59: 688-691, 1970

Fujita H: Diffusion in polymer-diluent systems. Fortschr Hoch-polym –Forsch 3: 1-47, 1961

Gabrielsson J, Lindberg N-O, Lundstedt T: Multivariate methods in pharmaceutical applications. J Chemometrics 16: 141-160, 2002

Gao P, Skoug JW, Nixon PR, Ju TR, Stemm NL, Sung K-C: Swelling of hydroxypropyl methylcellulose matrix tablets. 2. Mechanistic study of the influence of formulation variables on matrix performance and drug release. J Pharm Sci 85: 732-740, 1996

Geladi P, Kowalski BR: Partial least-squares regression: A tutorial. Anal Chim Acta 185: 1-17, 1986

Gillespie WR: Convolution-based approaches for in vivo-in vitro correlation modelling. Adv Exp Med Biol 423: 53-65. 1997

Göpferich A: Mechanism of polymer degradation and erosion. Biomaterials 17: 103-114, 1996

Habib YS, Shangraw RF: Effect of different drying techniques on the physico-mechanical properties of beads containing microcrystalline cellulose (mmc) produced by extrusion spheronization. Pharm Res 14: S14, 1997

Haleblian J, McCrone W: Pharmaceutical applications of polymorphism. J Pharm Sci 58: 911-929, 1969

Hamed E, Sakr A: Application of multiple response otimization technique to extended release formulations design. J Control Rel 73: 329-338, 2001

Harland RS, Gazzaniga A, Sangani ME, Colombo P, Peppas NA: Drug – polymer matrix swelling and dissolution. Pharm Res 5: 488-494, 1988

Heckel RW: Density pressure relationship in powder compaction. Trans Metall Soc AIME 221 (suppl a): 671-675, 1961a

Heckel RW: An analysis of powder compaction phenomena. Trans Metall Soc AIME. 221 (suppl b): 1001-1008, 1961b

Hintz RJ, Johanson KC: The effect of particle size distribution on dissolution rate and oral absorption. Int J Pharm 51: 9-17, 1989

Hubert HE, Dale LB, Christerson GL: Utilization of hydrophilic gums for the control of drug release from tablet formulation, I. Disintegration and dissolution behaviour. J Pharm Sci 55:974-976, 1966

Hussain N, Jaitley V, Florence AT: Recent advances in the understanding of uptake of microparticles across the gastrointestinal lymphatics. Adv Drug Deliv Rev 50: 107-142, 2001

Hörter D, Dressman JB: Influence of physicochemical properties on dissolution of drugs in the gastrointestinal tract. Adv Drug Deliv Rev 46: 75-87, 2001

Jounela A, Pentikainen P, Sothmann A: Effect of particle size on the bioavailablility of digoxin. Eur J Clin Pharmacol 8: 365-370, 1975

Jover I, Podczeck F, Newton M: Evaluation by a statistically designed experiment of an experimental grade of microcrystalline cellulose, Avicel 955, as a technology to aid the production of pellets with high drug loading. J Pharm Sci 85: 700-705, 1996

Ju RTC, Nixon PR, Patel MV: Drug release fron hydrophilic matrices. 1. New scaling laws for predicting polymer and drug release based on the polymer disentanglement concentration and diffusion layer. J Pharm Sci 84: 1455-1463, 1995a

Ju RTC, Nixon PR, Patel MV: Drug release fron hydrophilic matrices. 2. A mathematical model based on the polymer disentanglement concentration and the diffusion layer. J Pharm Sci 83: 1464-1477, 1995b

Ju RTC, Nixon PR, Patel MV: Diffusion coefficients of polymer chains in the diffusion layer adjacent to a swollen hydrophilic matrix. J Pharm Sci 86: 1293-1297, 1997

Karehill PG, Glazer M, Nyström C: Studies on direct compression of tablets. XXIII. The importance of surface roughness for compactability of some directly compressible materials with different bonding and volume reduction properties. Int J Pharm 64: 35-43, 1990

Karnachi AA, Khan MA: Box-behnken design for the optimization of formulation variables of indomethacin coprecipitates with polymer mixtures. Int J Pharm 131: 9-17, 1996

Kassem MA, Mattha AG, El-Nimr AEM, Omar SM: Study on the influence of sodium taurocholate (STC) and sodium glucocholate (SGC) on the mass transfer of certain drugs. Digoxin. Int J Pharm 12: 1-9, 1982

Kim CJ: Drug release from compressed hydrophilic POLYOX-WSR tablets. J Pharm Sci 84: 303-306, 1995

Kleinebudde P: Shrinking and swelling properties of pellets containing microcrystalline cellulose and low substituted hydroxypropylcellulose: I. Shrinking properties. Int J Pharm 109: 209-219, 1994

Korsmeyer RW, Gurny R, Doelker EM, Buri P, Peppas NA: Mechanism of solute release from porous hydrophilic polymers. Int J Pharm 15: 25-35, 1983

Lapidus H, Lordi NG: Some factors affecting the release of a water-soluble drug from a compressed hydrophilic matrix. J Pharm Sci 55: 840-843, 1966

Lapidus H, Lordi NG: Drug release from compressed hydrophilic matrices: J Pharm Sci 57: 1292-1301, 1968

Lee PI: Diffusional release of a solute from a polymeric matrix-approximate analytical solutions. J Membrane Sci 7: 255-275, 1980

Lee PI, Peppas NA: Prediction of polymer dissolution in swellable controlled-released systems. J Control Rel 6: 207-215, 1987

Lee PI, Kim CJ: Probing the mechanisms of drug release from hydrogels. J Control Rel 16: 229-236, 1991

Lindberg N-O, Lundstedt T: Multivariate data analysis of variables influencing the dissolution rate of prednimustine: A case of disconformity with the Noyes-Whitney equation. Eur J Pharm Biopharm 41: 1014-113, 1995

Loo J, Riegelman S: New method for calculating the intrinsic absorption rate of drugs. J Pharm Sci 57: 918-928, 1968

Ludde KH, Kawakita K: Die pulverkompression. Pharmazie 21: 393-403, 1966

Luner PE, Babu SR, Radebaugh GW: The effects of bile salts and lipids on the physicochemical behavior of gemfibrozil. Pharm Res 11: 1755-1760, 1994

Macheras P, Reppas C, Dressman JB: Estimation of volume/flow ratio of gastrointestinal (GI) fluids in humans using pharmacokinetic data. Pharm Res 7: 518-522, 1990

Malamataris S, Karidas T: Effect of particle size and sorbed moisture on the tensile strength of some tableted hydroxypropyl methylcellulose (HPMC) polymers. Int J Pharm 104: 115-123, 1994

Mallapragada SK, Peppas NA: Crystal unfolding and chain disentanglement during semicrystalline polumer dissolution. AIChe J 43: 870-876, 1997

Martin A: Diffusion and Dissolution. In: Physical Pharmacy, pp. 324-361. Eds. A Martin, Lea & Febiger, Malvern, Pennsylvania, USA, 1993

Menon AS, Mujumdar AS: Drying of solids: Principles, Classification, and selection of dryers. In: Handbook of Industrial Drying, pp. 3-46. Eds. AS Mujumdar, Marcel Dekker Inc., New York, NY, USA, 1987

Mithani SD, Bakatselou V, Tenhoor CN, Dressman JB: Estimation of the increase in solubility of drugs as a function of bile salt concentration. Pharm Res 13: 163-167, 1996

Moore JG: Horizontal vacuum rotary dryers. In: Handbook of Industrial Drying, pp. 155-164. Eds. AS Mujumdar, Marcel Dekker Inc., New York, NY, USA, 1987

Munoz-Ruiz A, Paronen P: Time-dependent densification behaviour of cyclodextrins. J Pharm Pharmacol 48: 790-797, 1996

Möckel JE, Lippold BC: Zero-order drug release from hydrocolloid matrices. Pharm Res 10: 1066-1070, 1993

Narasimhan B, Peppas NA: Disentanglement and reptation during dissolution of rubbery polymers. J Polym Sci Polym Phys 34: 947-961, 1996a

Narasimhan B, Peppas NA: On the importance of chain reptation in models of dissolution of glassy polymers. Macromolecules 29: 3283-3291, 1996b

Narasimhan B, Peppas NA: Molecular analysis of drug delivery systems by dissolution of the polymer carrier. J Pharm Sci 86: 297-304, 1997a

Narasimhan B, Peppas NA: The physics of polymer dissolution: modelling approaches and experimental behavior. Adv Polym Sci 128:157-207, 1997b

Narasimham B: Accurate models in controlled drug velivery systems. In: Hanbook of pharmaceutical controlled release technology, pp. 155-188. Eds. DL Wise, Marcel Dekker, New York, NY, USA, 2000

Narasimhan B: Mathematical models describing polymer dissolution: consequences for drug delivery. Adv Drug Deliv Rev 48: 195-210, 2001

Nokhodchi A, Rubinstein MH: Ford JL. The effect of particle size and viscosity grade on compaction properties of hydroxymethylcellulose 2208. Int J Pharm 126: 189-197, 1995

Norris DA, Puri N, Sinko PJ: The effect of physical barriers and properties on the oral absorption of particulates. Adv Drug Deliv Rev 34: 135-154, 1998

Noyes AA, Whitney WR: Über die auflösungsgeschwindigkeit von festen Stoffen in ihren eigenen Lösungen. Z Physik Chemie 13: 689-692, 1897

Nyström G, Aldernborn G, Duberg M, Karehill PG: Bonding surface area and bonding mechanisms - two important factors for the understanding of powder compactability. Drug Dev Ind Pharm 19: 2143-2196, 1993

O'Hara TO, Hayes S, Davis J, Devane J, Smart T, Dunne A: *In vivo-in vitro* correlation (IVIVC) modeling incorporating a convolution step. J Pharmacokin Pharmacodyn 28: 277-298, 2001

Ovensen L, Bentsen F, Tage-Jansen U, Pedersen NT, Gram BR, Rune SJ: Interluminal pH in the stomach, duodenum, proximal jejunum in normal subjects and patients with exocrine pancreatic insufficiency. Gastroenterol 90: 958, 1986

Ozturk SS, Palsson BO, Dressman JB: Dissolution of ionisable drugs in buffered and unbuffered solutions. Pharm Res 5: 272-282, 1988

Paronen PT, Peltonen SH, Urtti AO, Nakari LJ: Starch acetate composition with modifiable properties, method for preparation and usage thereof. US. Patent. 5.667.803, 1997

Peppas NA, Franson NM: The swelling interface number as a criterion for prediction of diffusion solute release mechanism in swellable polymers. J Polym Sci Polym Phys 121: 983-997, 1983

Peppas NA, Gurny R, Doelker E, Buri P: Modelling of drug diffusion through swellable polymeric systems. J Membrane Sci 7: 255-275, 1980

Pinto FJ, Podczeck F, Newton JM: Investigations of tablets prepared from pellets produced by extrusion and spheronisation. Part I: The application of canonical analysis to correlate the properties of tablets to the factors studied in combination with principal component analysis to select the most relevant factors. Int J Pharm 147: 79-93, 1997

Pohja S, Suihko E, Vidgren M, Paronen P, Ketolainen J: Starch acetate as a tablet matrix for sustained drug release. (in press: J Contro. Rel), 2003

Proost JH: Application of a numerical deconvolution technique in the assessment of bioavailability. J Pharm Sci 74: 1135-1136, 1985

Qiu Y, Samara EE, Cao G: Vitro – In Vivo correlations in the development of solid oral controlled release dosage forms. In: Handbook of pharmaceutical controlled release technology. Vol. 1. pp. 527-549. Eds. DL Wise, Marcel Dekker Inc., New York, NY, USA, 2000

Qiu Y, Zhang G: Research and development aspects of oral controlled-release dosage forms. In: Handbook of pharmaceutical controlled release technology. Vol. 1. pp. 465-504. Eds. DL Wise, Marcel Dekker Inc., New York, NY, USA, 2000

Raatikainen P, Korhonen O, Peltonen S, Paronen P: Acetylation Enhances the Tabletting Properties of Starch. Drug Dev Ind Pharm 28, 165-175, 2002

Ragnarsson G, Sjögren J: Work of friction and net work during compaction. J Pharm Pharmacol 35: 201-204, 1983

Ragnarsson G, Sjögren J: Force displacement measurement in tableting. J Pharm Pharmacol 37: 145-150, 1985

Rasool AA, Hussain AA, Ditter LW: Solubility enhancement of some water-insoluble drugs in the presence on nicotinamide and relates compounds. J Pharm Sci 80: 387-393, 1991

Remon JP, Schwartz JB: Effect of raw materials and processing on the quality of granules prepared from microcrystalline cellulose-lactose mixtures. Drug Dev Ind Pharm 13: 1-14, 1987

Reppas C, Meyer JH, Sirois PJ, Dressmann: Effect of hydroxypropylmethylcellulose on gastrointestinal transit and luminal viscosity in dogs. Gastroenterol 100: 1217-1223, 1991

Ritger PL, Peppas NA: A simple equation for description of solute release I. Fickian and non-Fickian release from non-swellable devices in the form of slabs, spheres cylinders or discs. J Control Rel 5: 23-36, 1987

Russel TL, Berardi RR, Barnett JL, Dermentzoglou LC, Jarvenpaa KM, Schmaltz SP, Dressman JB. Upper gastrointestinal pH in 79 healthy, elderly, North American men and women. Pharm Res 10: 187-196, 1993

Sastry SV, Reddy IK, Khan MA: Atenolol gastrointestinal therapeutic system: optimisation of formulation variables using response surface methodology. J Control Rel 45: 121-130, 1997

Schinkel AH, Jonker JW: Mammalian drug efflux transporters of the ATP binding cassette (ABC) family: An overview. Adv Drug Deliv Rev 55: 3-29, 2003

Sharma VK: Comparison of 24-hours intragastric pH using four liquid formulations of lansoprazole and omeprazole. Am J Health Syst Pharm 56(23 Suppl 4): S18-21, 1999

Shefter E, Higuchi T: Dissolution behavior of crystalline solvated and non-solvated forms of some pharmaceuticals. J Pharm Sci 52: 781-791, 1963

Siepmann J, Kranz H, Bodmeier R, Peppas NA: HPMC-matrices for controlled drug delivery: A new model combining diffusion, swelling and dissolution mechanism and predicting the release kinetics. Pharm Res 16: 1748-1756, 1999a

Siepmann J, Podual K, Sriwongjanya M, Peppas NA, Bodmeier R: A new model describing the swelling and drug release kinetics from hydrpxypropyl ethylcellulose tablets. J Pharm Sci 88: 65-72, 1999b

Siepmann J, Kranz H, Peppas NA, Bodmeier R: Calculation of the required size and shape of hydroxypropyl methylcellulose matrices to achieve desired drug release profiles. Int J Pharm 201: 151-164, 2000a

Siepmann J, Peppas NA: Hydrophilic matrices for controlled drug delivery: An important mathematical model to predict the resulting drug release kinetics (the "sequential layer" model). Pharm Res 17: 1290-1298, 2000b

Siepmann J, Peppas NA: Modeling of drug release from delivery systems based on hydroxypropyl methylcellulose (HPMC). Adv Drug Deliv Rev 48: 139-157, 2001

Siepmann J, Streubel, Peppas NA: Understanding and predicting drug delivery from hydrophilic matrix tablets using the "Sequental Layer" model. Pharm Res 19: 306-314, 2002

Singer SJ, Nicolson GL: The fluid mosaic model of the structure of cell membranes. Science 175: 720-731, 1972

Steendam R, Eissens ACE, Frijlink HW, Lerk CF: Plasticisation of amylodextrin by moisture consequences for drug release from tablets. Int J Pharm 204: 23-33, 2000

Stouch TR, Gudmundsson O: Progress in understanding the structure-activity relationship of P-glycoprotein. Adv Drug Deliv Rev 54: 315-328, 2002

Strous GJ, Dekker J: Mucin-type Glycoproteins. Crit Rev Biochem Mol Biol 27: 57-92, 1992

Tahara K, Yamamoto K, Nishihata T: Overall mechanism behind matrix sustained release (SR) tablets prepared with hydroxypropyl methylcellulose 2910. J Control Rel 35: 59-66, 1995

Tahara K, Yamamoto K, Nishihata T: Application of model-independent and model analysis for the investigation of effect of drug solubility on its release rate from hydroxypropyl methylcellulose sustained release tablets. Int J Pharm 133: 17-27, 1996

Takayama K, Morva A, Fujikawa M, Hattori Y, Obata Y, Nagai T: Formula optimization of theophylline controlled-release tablet based on artificial neural networks. J Control Rel 68: 175-186, 2000

Talukdar MM, Kinget R: Comparative study on xanthan gum and hydroxypropyl methylcellulose as matrices for controlled-release drug delivery. II. Drug diffusion in hydrated matrices. Int J Pharm 151: 99-107, 1997

Tamada JA, Langer R: Erosion kinetics of hydrolytically degradable polymers. Proc Natl Acad Sci 90: 552-556, 1993

Tanaka Y, Taki Y, Sakane T, Sezaki H, Yamashita S: Characterization of drug transport through tight-junctional pathway in Caco-2 monolayer: Comparison with isolated rat jejunum and colon. Pharm Res 12: 523-528, 1995

Tarvainen M, Sutinen R, Somppi M, Paronen P, Poso A: Predicting plasticization efficiency from three-dimensional molecular structure of a polymer plasticizer. Pharm Res 18: 1760-1766, 2001

Te Wierik GHP, Eissens AC, Bergsma J, Arends-Scholte AW, Bolhuis GK: A new generation starch products as excipient in pharmaceutical tablets III. Parameters affecting controlled drug release from tablets based on high surface area retrograded pregelanized potato starch. In J Pharm 157: 181-187, 1997

Tsuji A, Tamai I: Carrier-mediated intestinal transport of drugs. Pharm Res 13: 963-977, (1996)

Venkataraman S, Davar N, Chester A, Kleiner L: An overview of controlled release systems. In. Handbook of pharmaceutical controlled release technology. pp. 431-463. Eds. DL Wise, Marcel Dekker Inc., New York, NY, USA, 2000

Wagner JG: Pharmacokinetic absorption plots from oral data alone or oral/intravenous data and an exact Loo-Riegelman equation. J Pharm Sci 72: 838-842, 1983

Weber H, Steimer U, Mannhold R, Cruciani G: Synthesis, In Vitro skin permeation studies, and PLS-Analysis of new naproxen derivatives. Pharm Res 18: 600-607, 2001

Westerhuis JA, Coenegracht PMJ, Lerk CF: Multivariate modelling of the tablet manufacturing process with wet granulation for tablet optimisation and in-process control. Int J Pharm 156: 109-117, 1997

Wold S, Esbensen K, Geladi P: Principal component analysis. Chemometrics Intell Lab Syst 2: 37-52, 1987a

Wold S, Geladi P, Esbensen K, Öhman J: Multiway principal components and PLS-analysis. J Chemometrics 1: 41-56, 1987b

Wold S, Sjöström M, Erikkson L: PLS-regression: a basic tool of chemometrics. Chem Intell Lab Syst 58: 109-130, 2001

Wong LW, Pilpel N: The effect of particle shape on the mechanical properties of powders. Int J Pharm 59: 145-154, 1990

Wurzburg OB: Acetylation. In: Methods in Carbohydrate Chemistry, Volume IV, pp. 288. Eds. RL Whistler, Academic Press, New York, 1964

York P: Particle slippage and rearrangement during compression of pharmaceutical powders. J Pharm Pharmacol 30: 6-10, 1978

Yu L: Amorphous pharmaceutical solids: preparation, characterization and stability. Adv Drug Deliv Rev 48: 27-42, 2001

Zackrisson G, Östling G, Skagerberg B, Anfält T: Accelerated dissolution rate analysis (ACDRA) for controlled release drugs. Application to Roxiam. J Pharm Pharm Biomed Anal 13: 377-383, 1995

Österberg T, Norinder U: Prediction of drug transport processes using simple parameters and PLS statistics. The use of ACD/logP and ACD/ChemSketch descriptors. Eur J Pharm Sci 12: 327-337, 2001

8 ORIGINAL PUBLICATIONS

I Ossi Korhonen, Pasi Raatikainen, Päivi Harjunen, Johanna Nakari, Eero Suihko, Soili Peltonen, Mika Vidgren, Petteri Paronen: Starch Acetates - Multifunctional Direct Compression Excipients.
Pharmaceutical Research 17: 1138-1143, 2000

II Ossi Korhonen, Seppo Pohja, Soili Peltonen, Eero Suihko, Mika Vidgren, Petteri Paronen, Jarkko Ketolainen: Effects of Physical Properties for Starch Acetate Powders on Tableting.
AAPS Pharmaceutical Science & Technology 3(4), 2002

III Ossi Korhonen, Antti Poso, Mika Vidgren, Petteri Paronen, Seppo Pohja, Jarkko Ketolainen: PCA- and PLS-analyses in evaluating drug release from starch acetate matrix tablets.
European Journal of Pharmaceutical Sciences, 2003, Submitted

IV Ossi Korhonen, Harri Kanerva, Mika Vidgren, Arto Urtti, Jarkko Ketolainen: Administration of Novel Starch Acetate – Diltiazem Controlled Release Tablets to Healthy Human Volunteers.
Journal of Controlled Release, 2003, Accepted for publication